



HAL
open science

Unravelling mechanisms behind population dynamics, biological traits and latitudinal distribution in two benthic ecosystem engineers: A modelling approach

Lola de Cubber, Sébastien Lefebvre, Théo Lancelot, Daniel Schaffer Ferreira
Jorge, Sylvie Marylène Gaudron

► To cite this version:

Lola de Cubber, Sébastien Lefebvre, Théo Lancelot, Daniel Schaffer Ferreira Jorge, Sylvie Marylène Gaudron. Unravelling mechanisms behind population dynamics, biological traits and latitudinal distribution in two benthic ecosystem engineers: A modelling approach. *Progress in Oceanography*, 2023, 219, pp.103154. 10.1016/j.pocean.2023.103154 . hal-04272435

HAL Id: hal-04272435

<https://hal.science/hal-04272435>

Submitted on 6 Nov 2023

HAL is a multi-disciplinary open access archive for the deposit and dissemination of scientific research documents, whether they are published or not. The documents may come from teaching and research institutions in France or abroad, or from public or private research centers.

L'archive ouverte pluridisciplinaire **HAL**, est destinée au dépôt et à la diffusion de documents scientifiques de niveau recherche, publiés ou non, émanant des établissements d'enseignement et de recherche français ou étrangers, des laboratoires publics ou privés.

Unravelling mechanisms behind population dynamics, biological traits and latitudinal distribution in two benthic ecosystem engineers: a modelling approach

Lola De Cubber^{a,b,x}, Sébastien Lefebvre^a, Théo Lancelot^a, Daniel Schaffer Ferreira Jorge^a, Sylvie Marylène Gaudron^{a,c}

^aUniv. Lille, Univ. Littoral Côte d'Opale, CNRS, IRD, UMR 8187 Laboratoire d'Océanologie et de Géosciences, F-59000 Lille, France

^bMARBEC, Univ Montpellier, CNRS, IFREMER, IRD, Sète, France

^cSorbonne Univ., UFR 918, 75005 Paris, France

Abstract

The mechanistic approach consisting of coupling Dynamic Energy Budget (DEB) models to Individual-Based Models (IBMs) allows simulating individual and population biological traits and their dynamics. This approach was developed here to study population dynamics of two sympatric intertidal ecosystem engineers, *Arenicola marina* and *Arenicola defodiens* (Annelida Polychaeta) occurring in the North-East Atlantic from Portugal to Sweden. Latitudinal heterogeneity of the two species' performances were investigated in terms of population dynamics and biological traits using latitudinal differences in environmental forcing variables. The impact of the forcing variables on population dynamics processes (shore colonisation and migration, spawning and recruitment, etc.) within a specific foreshore (mean values and seasonal patterns) was also assessed. Published DEB parameters were used for *A. marina* and a specific calibration was undertaken for *A. defodiens*, combining literature data and new laboratory experiments and field data. Our DEB-IBM simulated super-individuals' growth and reproduction while lugworms were colonising, migrating and dying over a simulated foreshore. Density rules affected population dynamics. Environmental forcings consisted in monthly values of chlorophyll-a (chl-a) concentrations and daily values of SST. Scenarios focusing on the two most contrasted of these forcing variables time series were used to explore their relative effects over populations' dynamics and on-shore processes were investigated at two sites displaying highly different simulated population abundances. Overall, northern sites with higher chl-a levels performed better displaying higher biomass, maximum length and reproductive outputs for both species. As expected, Sea Surface Temperature (SST) changes between sites did not impact greatly populations dynamics. Under favourable environmental conditions, intra- and inter-specific competitions emerged from the model. Under non-favourable environmental conditions, *A. defodiens*' populations crashed and *A. marina* displayed atypical population processes, with rare spawning events barely allowing the population's renewal, and lower size at maturity. Further use and development of this model will lead to better insights on the lugworm populations' evolution over the next decades.

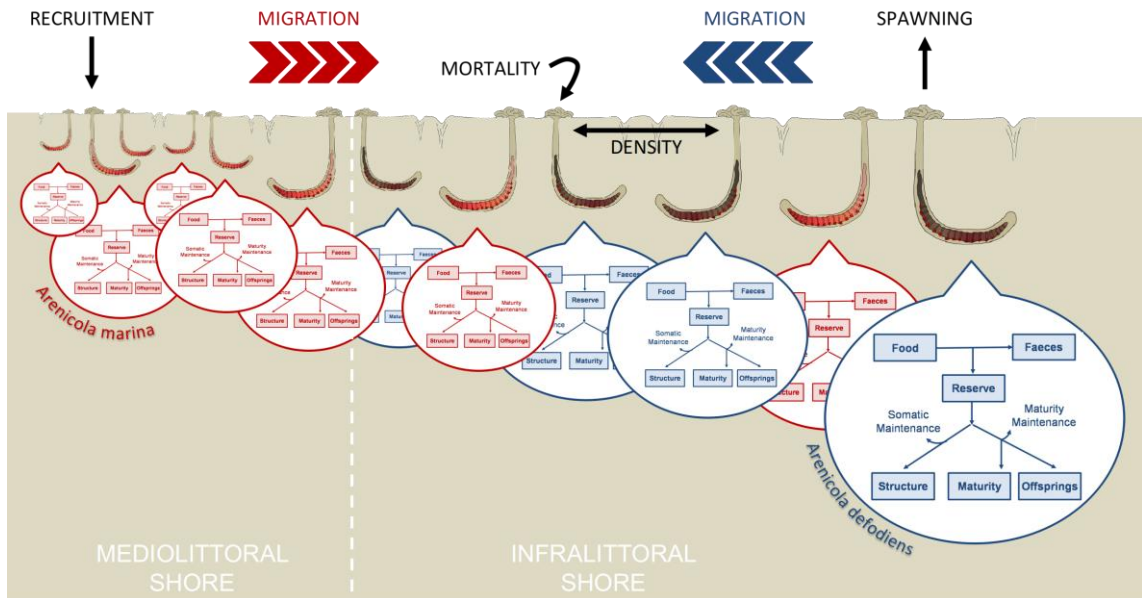
^xCorresponding author: lola.decubber@gmail.com

1
2
3
4
5
6
7
8
9
10
11
12
13
14
15
16
17
18
19
20
21
22
23
24
25
26
27
28
29
30
31
32
33
34
35
36
37
38
39
40
41
42
43
44
45
46
47
48
49
50
51
52
53
54
55
56
57
58
59
60
61
62
63
64
65

36 **Key words**

37 Dynamic Energy Budget model, Individual-Based Model, *Arenicola marina*, *Arenicola defodi-*
38 *ens*, North-East Atlantic

39 **Graphical abstract**



Graphical representation of the DEB-IBM developed in this study. Individuals from two species of lugworms displaying different shore colonisation patterns are followed. Their length, reproduction rate and development are obtained from DEB models, and other population processes are considered (e.g. mortality, predation) on a simulated shore where density is a limiting factor.

40 **Highlights**

- 41 • A Dynamic Energy Budget - Individual-Based Model was developed for two benthic poly-
42 chaetes
- 43 • Population dynamics were simulated under environmental condition recovered from Portugal
44 to Sweden
- 45 • Northern sites with higher chl-a levels performed better (higher biomass and maximum
46 length)
- 47 • Under favourable conditions, intra- and inter-specific competition emerged from the model
- 48 • Under non-favourable conditions, *A. defodiens*' populations crashed

1. Introduction

Coastal ecosystems are subject to many and intensifying anthropogenic pressures (Halpern et al., 2015) and therefore require a better understanding of their functioning and biodiversity dynamics, which is becoming a growing challenge for marine ecologists (Mangano et al., 2020; Thomas and Bacher, 2018; Harley et al., 2006). In the context of global change, correlative niche models linking population dynamics processes such as survival or reproduction rates to a set of environmental variables might lead to poor predictive power when transferred to novel environments (Davis et al., 1998). As a consequence, a number of population dynamics approaches have been developed in order to explain and predict how biodiversity reacts to the environmental variability or to anthropogenic pressures (Batabyal, 1996; Caswell, 2001; Coulson, 2012; Grimm, 1999; Holmes et al., 1994; Huston et al., 1988; Picard and Liang, 2014). Overall, these models consist in studying the changes in numbers and size or age-structure of a population through time and space of a single species or more rarely of several species populations occurring as a consequence of population level processes including death (natural death or linked to predation, disease or harvesting) and the arrival of new individuals (via larval dispersal or migration, Wethey et al., 2011). However, these models are generally based on statistical correlations and not on a mechanistic understanding of the individual (physiological and behavioural) and population processes (inter-individual variability, dispersal and migrations) at stake (Kearney et al., 2010).

In order to address this issue, mechanistic models based on the knowledge of the physiological, phenological, behavioural or other responses of organisms to environmental variables have been developed (Malishev et al., 2017; Thomas and Bacher, 2018; Martin et al., 2012). They constitute promising tools for predicting species responses to climate change and understanding the mechanisms behind those responses. Among these approaches, Dynamic Energy Budget (DEB) models have been associated to Individual Based Models (IBM) to predict population dynamics and address a variety of ecological questions ranging from ecotoxicology (David et al., 2019; Beaudouin et al., 2012), fish ecology and fisheries management (Haberle et al., 2023), aquaculture (Bacher and Gangnery, 2006), and the study of potential impacts of climate change (Thomas and Bacher, 2018; Thomas et al., 2020). Dynamic Energy Budget (DEB) models simulate the effect of changing environmental conditions on the individuals' bioenergetics by quantifying the energy allocation to reserve, growth, maturation, reproduction and maintenance of a species at the individual level throughout its life cycle, thus providing predictions of growth, reproduction and life-history traits of individuals according to environmental conditions such as temperature and food availability (Kooijman, 2010). Over the last 25 years, the theory has kept expanding and models based on the DEB theory have been applied to over 3000 species with a wide variety of applications (https://www.bio.vu.nl/thb/deb/deblab/add_my_pet/). Combined with agent-based or IBMs that focus on individual processes in order to understand higher levels of biological complexity such as population dynamics (De Angelis and Grim, 2014), they enable estimating

1
2
3
4
5
6
7
8
9
10
11
12
13
14
15
16
17
18
19
20
21
22
23
24
25
26
27
28
29
30
31
32
33
34
35
36
37
38
39
40
41
42
43
44
45
46
47
48
49
50
51
52
53
54
55
56
57
58
59
60
61
62
63
64
65

86 the impact of varying environmental conditions not only at the individual level but also at the
87 population level (Kearney et al., 2009; 2010; Malishev et al., 2017; Thomas and Bacher, 2018). In
88 practice, single individuals can be followed, or populations are divided into a number of cohorts
89 followed as discrete entities. In the latter case, cohorts are treated individually as super-individuals
90 with the same DEB state variables. Each super-individual can contain all individuals from a given
91 age cohort, integrating inter-individual variability, or a given number of individuals with the same
92 properties and no inter-individual variability. New cohorts can be generated depending on the
93 reproductive status of the followed cohorts (Pethybridge et al., 2013; Thomas and Bacher, 2018).
94 Functional traits can then be extracted from the obtained population dynamics (Mangano et al.,
95 2019). Functional traits are “morphological, biochemical, physiological, structural, phenological,
96 or behavioural characteristics of organisms that influence how they respond to the environment
97 (response traits) and/or their effects on ecosystem properties (effect traits)” (Violle et al., 2007).
98 The comparison of response traits (for example biomass or reproductive output) can help identify-
99 ing optimal environmental conditions for a given species and scenario-specific quantitative maps of
100 biomass or reproductive output can then be considered to inform fisheries management (Mangano
101 et al., 2019). As an example, the identification of areas with predicted high abundance can help
102 defining protection areas (Mangano et al., 2020). The most common biological population response
103 traits generally used are linked with population and individual growth (abundance, biomass and
104 maximum length of individuals) and reproduction (total reproductive output and length at first
105 maturity) (Mangano et al., 2020).

106 Here, we used DEB-IBM to study the population dynamics and biological traits of two widespread
107 engineer species, the lugworm *Arenicola marina* (Linnaeus, 1758) and the black lugworm *Arenicola*
108 *defodiens* (Cadman and Nelson-Smith, 1993) along the North-East Atlantic coast. Among the
109 species diversity within ecosystems, engineer species possess functional traits that largely and non-
110 linearly influence their surrounding environment, providing key ecosystem functions and services
111 such as nutrient recycling or ecosystem resilience and stability (see Yeakel et al., 2020; Wrede et
112 al., 2019). *A. marina* and *A. defodiens* are psammivorous benthic polychaetes (Annelida) inhab-
113 iting sandy shores on the Eastern Atlantic coast from Portugal to the Arctic (Pires et al., 2015;
114 Volkenborn, 2005). Both species live within galleries dug in the sediment up to 30 to 40 cm deep
115 for *A. marina* and up to 70 cm deep for *A. defodiens*. They ingest the superficial (for *A. marina*)
116 or deeper (for *A. defodiens*) sediment to feed on the organic matter it contains, and create a wa-
117 ter current bringing oxygen to their gills and tegument (Cadman and Nelson-Smith, 1993; Senga
118 Green et al., 2016). This bioturbation modifies the abiotic conditions within the sediment (grain
119 size, nitrogen and oxygen content) and impacts the associated communities’ composition, enhanc-
120 ing selected species at the expense of others (Clarke et al., 2017; Kristensen, 2001; Reise, 1985;
121 Volkenborn, 2005). Records of their shore distribution showed that they can live separately occu-
122 pying different bathymetric levels on the same shore or in sympatry on the same bathymetric level

1
2
3
4
5
6
7
8
9
10
11
12
13
14
15
16
17
18
19
20
21
22
23
24
25
26
27
28
29
30
31
32
33
34
35
36
37
38
39
40
41
42
43
44
45
46
47
48
49
50

123 (Cadman, 1997; De Cubber et al, 2018). Apart from their ecological role, the species are still used
124 as baits and commonly harvested in Europe (UK, France, the Netherlands, etc.) by professional
125 and recreational fishermen (Watson et al., 2017). Over-exploitation of these species has long been
126 feared and reported (Blake, 1979; Olive, 1993) and confirmed recently in some areas (De Cubber et
127 al., 2018), potentially leading to changes in size and age structure, abundance and distribution of
128 local populations. Conversely, in Southern Europe, their expansion has been reported locally and
129 might impact other native species with high ecological value such as the eelgrass, *Zostera noltii*
130 (Pires et al., 2015). Our interest was thus to be able to simulate population dynamics at both a
131 small local (foreshore scale) and a wide (North-East Atlantic coast) scale to then be able to address
132 the questions around the local differences of shore distribution, the local impacts of harvesting on
133 single shores and the possible environmental change effects on overall latitudinal distributions.

134 Physiology and behaviour of the two species have been studied unevenly. *A. marina* individ-
135 ual responses to different environmental conditions have already been simulated with a Dynamic
136 Energy Budget model (De Cubber et al., 2019; 2020). The study showed that Sea-Surface Tem-
137 perature (SST) and planktonic Chlorophyll-a concentration (chl-a) are relevant forcing variables to
138 properly simulate the species response to environment (De Cubber et al., 2020). The down-shore
139 migration of *A. marina* individuals while growing has also already been documented (De Cubber
140 et al., 2020), and the future distribution trends investigated with age-structured meta-population
141 models considering varying mortality rates according to heat waves (Wethey and Woodin, 2022).
142 Nevertheless, no study representing expressively the mechanisms influencing the species dynam-
143 ics and survival were developed until now to our knowledge. *A. defodiens* was much less studied
144 and few data are available regarding the species individual and population traits, and hence the
145 potential interaction (in terms of spatial competition) between both species.

146 We used spatially explicit forcing variables to drive DEB models at the individual scale to
147 simulate the life-history traits at the population scale of two lugworm's species, *A. marina* and *A.*
148 *defodiens* (i.e. growth and reproduction) as a function of environmental variables (i.e. SST and
149 chl-a). We then integrated each DEB model into a individual-based density-dependent population
150 dynamic model (DEB-IBM, Martin et al., 2012) and applied the DEB-IBM to a number of locations
151 in Europe where the two polychaetes species have been already studied on a latitudinal gradient
152 during the period 2010-2020. Our main objectives were:

- 153
- 154 1. To develop a two-species DEB-IBM reflecting the most comprehensive way processes involved
155 into the species population dynamics, namely: the generation of new individuals (or super
156 individuals) based on reproduction, the variability of some model parameters, the mobility
157 and habitat preferences of the individuals and mortality;
 - 158 2. To simulate potential latitudinal discrepancies between lugworm populations in terms of pop-
159 ulation dynamics and biological traits (length at puberty, maximum body size, size distribu-
tion, biomass, abundance and total reproductive output) explained by latitudinal differences

1
2
3
4
5
6
7
8
9
10
11
12
13
14
15
16
17
18
19
20
21
22
23
24
25
26
27
28
29
30
31
32
33
34
35
36
37
38
39
40
41
42
43
44
45
46
47
48
49
50
51
52
53
54
55
56
57
58
59
60
61
62
63
64
65

160 in environmental forcings;

- 161 3. To understand the impact of the two forcing factors (temperature and chl-a) on population
162 dynamics processes (shore colonisation and migration, spawning and recruitment, etc.) of
163 the two lugworm species within a specific foreshore (mean values, inter-annual and seasonal
164 patterns).

165 **2. Material and Methods**

166 *2.1. Dynamic Energy Budget Models*

167 *2.1.1. Description*

168 *DEB models and lifecycle.* The DEB theory describes the energy flows within an organism between
169 three compartments (state variables): the reserve (E), the structure (V), and the maturity (E_H)
170 or the reproduction buffer (offsprings) (E_R) according to its life stage in order to describe its
171 energy allocation to growth, reproduction and maintenance for a given food level and at a reference
172 temperature T_{ref} (Kooijman, 2010). The DEB model equations for *A. marina* and the link between
173 the model and the species' lifecycle have already been described by De Cubber et al. (2019; 2020)
174 (see Table 1).

175 Briefly, both lugworm species exhibit annual iteroparity (Watson et al., 2000). Populations of
176 *A. marina* have been reported to spawn epidemically over a few days to two weeks from September
177 to November depending on the targeted populations (Luttikhuisen and Dekker, 2010; Howie, 1984;
178 Watson et al., 2000). After spawning, non-feeding trochophore larvae of *A. marina* disperse to
179 a subtidal temporary habitat where they start feeding on deposited and suspended particles and
180 experience a metabolic acceleration (e.g the acceleration of all metabolic rates, see Kooijman,
181 2014) until the end of metamorphosis. After metamorphosis, the post-larval stages (juvenile stage)
182 will disperse again in the water column and recruit on the high mediolittoral sandy foreshores,
183 acquiring the psammivorous feeding behaviour of adults in spring to early summer. At this point,
184 metabolic acceleration ceases and juveniles will gradually migrate lower on the shore and reach
185 sexual maturation (puberty stage) (Sup. Mat. 1, De Cubber et al., 2019). Given the really
186 close phylogenetic relationship between *A. marina* and *A. defodiens*, the same abj-DEB model
187 (accounting for metabolic acceleration between the first feeding and the end of metamorphosis)
188 was used for both species with two different sets of parameters (see De Cubber et al., 2019;
189 2020). The lifecycle of *A. defodiens* in a natural environment has barely been described, except
190 for spawning events that have been reported from mid-December to early January (De Cubber et
191 al., 2018; Watson et al., 1998). However, based on *in situ* pers. observations (the authors and M.
192 Crouvoisier), we have made the hypothesis that individuals of *A. defodiens* disperse and recruit in
193 subtidal muddy habitats, and gradually reach infralittoral soft bottoms when reaching their sexual
194 maturity (see Sup. Mat. 1).

Table 1: Summary of the mathematical expressions used to build the Dynamic Energy Budget Individual-Based model (see Kooijman, 2010; De Cubber et al., 2020 for further details on the DEB models for *A. marina* and *A. defodiens*). DEB and IBM parameters are detailed in Table 2. L is the structural length (cm) with $L \propto V^{1/3}$, and L_b and L_j are the structural lengths at birth and metamorphosis respectively. a_j is the age at metamorphosis. TTR is the temperature tolerance range of the species. GSI is the wet weight of gametes divided by the total wet weight and $GSI_{trigger}$ the GSI leading to spawning. x_i is the shore level of individual i and $x_{subtidal}$ the shore level assigned to subtidal environment. d_x and $d_{max,x}$ are respectively the density at x and the maximum possible density at x . $bath$ is the bathymetry theoretically occupied by a lugworm according to its trunk length TL_w (De Cubber et al., 2020). $Capacity_{shore}$ is the shore capacity in terms of abundance of lugworms, calculated according to the max density per shore level. $N_{Offspring,emitted,i}$ is the number of offspring spawned per female, among which a (reduced) number $M_{Offspring,shore,i}$ offspring are simulated. RO_i is the reproductive output of individual i . Wx stands for Wimereux (East English Channel, France).

Dynamic Energy Budget Model equations		
Reserve		$\frac{dE}{dt} = \rho_A - \beta_C$
Structure		$\frac{dV}{dt} = \beta_G$
Maturity		$\frac{dE_H}{dt} = \alpha_{EH} \frac{rEGS}{E_H} \frac{dE_H}{dt} - \rho_H$; else $\frac{dE_H}{dt} = 0$
Reproduction		$\frac{dE_R}{dt} = \kappa_R - \beta_R$; else $\frac{dE_R}{dt} = 0$
Ingestion		$\beta_X = \frac{\beta_A}{K_X}$
Assimilation Mobilisation		$\beta_A = \frac{\beta_{AmU} \cdot S_M \cdot f \cdot V^{2/3}}{\beta \cdot S_M \cdot V^{2/3} + rEGS + \beta_S}$ $\beta_C = E \cdot \frac{\kappa \cdot E \cdot V + rEGS}{\kappa \cdot E \cdot V + rEGS}$
Somatic maintenance		$\beta_S = r\beta_{MS} \cdot V$
Maturity maintenance		$\beta_J = k_J \cdot E_H$
Growth		$\beta_G = \kappa \cdot \beta_C + \beta_S$
Reproduction		$\beta_R = p1 \cdot \kappa_q \cdot \beta_C + \beta_J$
Maturity		$\beta_H = p1 \cdot \kappa_q \cdot \beta_C + \beta_J$
Physical length (cm)		$L_w = ptq \cdot \frac{V^{1/3}}{\delta}$
Wet weight (g)		$W_w = ptq \cdot d_v \cdot V + ptq \cdot pEptq \cdot E_R + ptq \cdot \frac{wEd}{\mu Ed} \cdot dE$
Reproduction buffer handling rules	<i>A. marina</i> <i>A. defodiens</i>	if $(\Delta S_{T14} \leq 1^\circ C$ and $GSI \leq 0.1 \cdot W_w \cdot GSI_{trigger} \cdot W_w)$, spawn (set $E_R = 0$) if (day = 15 th of December), spawn (set $E_R = 0$)
Acceleration coefficient		if $E_H \leq E_H^b \cdot S_M = 1$; if $E_H^b \cdot d' E_H \leq E_H^j \cdot S_M = L\{L_b\}$; else $S_M = L_j\{L_b\}$ if $E_H \leq E_H^j$
Shape coefficient		if $E_H \leq E_H^b \cdot \delta = \delta$; if $E_H^b \cdot d' E_H \leq E_H^j \cdot \delta = \delta$; $p\delta \cdot \delta \cdot q = p \cdot \frac{L}{L_b} \cdot q$; else $\delta = \delta$ if $E_H \leq E_H^j$
Arrhenius temperature		$k_p T_q = k_1 \cdot \exp \frac{U_{ref}}{T_A} \cdot T_A^{-1} \cdot \exp \frac{T}{T_A} - \frac{T_{ref}}{T_A} \cdot \exp \frac{T_{ref}}{T_A}$
Scaled functional response		$f = \frac{X}{X + X_K} \cdot \exp \frac{T}{T_L} \cdot \exp \frac{T_{AH}}{T_{AH}} - \frac{T_{ref}}{T_{ref}}$
Inter-individual variability		$\beta_{AmU} = \beta_{AmU} \cdot e^{random\ normal(0, sd)}$, $\delta = \delta \cdot e^{random\ normal(0, sd)}$ and $\kappa = \kappa \cdot e^{random\ normal(0, sd)}$ with random normal(0, sd) a normally distributed (mean 0 and standard deviation sd) random number
Individual-Based Model rules and equations		
Migration rules	<i>A. marina</i>	if $E_H \leq E_H^j$ lugworm in subtidal area $x = x_{subtidal}$ if $E_H > E_H^j$ lugworm recruits on the higher 20% of higher mediolittoral shore $d_x d' d_{max,x}$ if $E_H > E_H^j$ $bath = 0.29 \cdot TL_{w,i} \cdot 6.60$, if $(x_i \geq bath_i$ and $d_x d' d_{max,x})$, set $x_i = bath_i$
Migration rules	<i>A. defodiens</i>	if $E_H \leq E_H^p$ black lug in subtidal area $x = x_{subtidal}$ if $E_H > E_H^p$ if $d_x d' d_{max,x}$, black lug moves to random x_i within infralittoral if $E_H > E_H^p$ $x_{i,t+1} = x_{i,t}$
Offspring number		$N_{Offspring,emitted,i} = ratio_i \cdot \frac{E_{R,i}}{E_0}$, if $Capacity_{shore} \leq \frac{x_{abundance}}{i^{n1}} N_{Offspring,emitted,i}^{aj}$ $N_{Offspring,shore,i} = N_{Offspring,emitted,i} \cdot s^{qj}$, else $N_{Offspring,shore,i} = \frac{Capacity_{shore} \cdot Abundance}{N_{spawning}}$ $a_j = 120$ for <i>A. marina</i> and $a_j = 110$ for <i>A. defodiens</i> , guessed from simulations at Wx
Individual-Based Model outputs analyses		
Abundance	<i>Abundance</i> (N indiv.)	<i>Abundance</i> _{marina} = count(<i>A. marina</i>), <i>Abundance</i> _{defodiens} = count(<i>A. defodiens</i>)
Total stock biomass	<i>TSB</i> (g)	<i>TSB</i> = $\sum_{i=1}^n W_{w,i}$, with n the abundance in <i>A. marina</i> or <i>A. defodiens</i>
mean Length at puberty	<i>L_{p,population}</i> (cm)	<i>L_{p,population}</i> = mean(<i>L_{p,individual}</i>)
Maximum length	<i>L_{max,population}</i> (cm)	<i>L_{max,population}</i> = mean(<i>L_{max,10%}</i> largest individuals)
Total reproductive output	<i>TRO</i> (N eggs)	<i>RO</i> = $\sum_{i=1}^{end\ simulation} N_{Offspring,emitted,t}$, <i>TRO</i> = $\sum_{i=1}^{N_{simulated\ individuals}} RO_i$
Gravity center of Y	<i>G_Y</i> (m of shore level)	<i>G_Y</i> = $\frac{\sum_{x=x_{min}}^{x_{max}} Y_x \cdot X}{Y}$, Y being the abundance or biomass, x the shore level

1
2
3
4
5
6
7
8
9
10
11
12
13
14
15
16
17
18
19
20
21
22
23
24
25
26
27
28
29
30
31
32
33
34
35
36
37
38
39
40
41
42
43
44
45
46
47
48
49
50
51
52
53
54
55
56
57
58
59
60
61
62
63
64
65

195 *Metabolic responses to food and temperature of A. marina.* In order to account for the impact of
196 environmental changes on the individuals' metabolism, corrections were made to the rates consid-
197 ered by the model in the equation of fluxes in terms of temperature and food quantity through
198 the Arrhenius temperature and the scaled functional response corrections (Kooijman, 2010, Table
199 1). The metabolic response to food and temperature of *A. marina* has already been explored (De
200 Cubber et al., 2020). The previous study identified the Arrhenius temperature of *A. marina* within
201 and outside the species temperature tolerance range, and the chlorophyll-a concentration as a good
202 proxy for food, with an associated half-saturation coefficient X_K of $5 \mu\text{g.L}^{-1}$ (De Cubber et al.,
203 2020).

204 *Metabolic responses to food and temperature of A. defodiens.* The effect of temperature on metabolic
205 rates of *A. defodiens* was extrapolated from an oxygen consumption experiment performed on 300
206 individuals of *A. defodiens* sampled at Wimereux ($50^{\circ}45'N$, $1^{\circ}36'E$) from May to July 2019. To
207 do so, a microelectrode Unisense® OX500 coupled to a picoammeter (Unisense PA 2000, Den-
208 mark) following De Cubber et al. (2019) with 325 ml containers filled with twice-filtered seawater
209 (TFSW) and with 500 ml containers half-filled with burnt sediment and the rest with TFSW. Five
210 temperatures were tested (10, 13, 16, 20 and $24^{\circ}C$) in these two treatments on 30 individuals per
211 treatment, where lugworms were acclimated 24h prior each respiration measurement. As no *in situ*
212 growth could be followed for this species in order to reconstruct the scaled functional response of
213 the species and identify a relevant proxy for food (De Cubber et al., 2020), the same proxy for
214 food and half-saturation coefficient X_K as for *A. marina* were used as a first approximation.

215 *Inter-individual variability.* Inter-individual variability was introduced following Martin et al. (2013)
216 and Koch and De Schampelaere (2020). A subset of 3 DEB parameters ($t_{A,m}$, κ and δ) were
217 considered to follow a normal distribution of the mean estimated value of parameter and stan-
218 dard deviation of 15%, taken from Koch and De Schampelaere (2020) and leading to relevant
219 size distributions within the population of Wimereux (Eastern English Channel, France). From the
220 original subset of parameters used by Martin et al. (2012), the maturity energy thresholds were
221 removed following Koch and De Schampelaere (2020) while the shape coefficient was added as it
222 is variable between individuals (see De Cubber et al., 2019; 2020) (Table 1).

223 2.1.2. DEB parameters estimation for *A. defodiens*

224 *A. defodiens'* DEB parameters were estimated using the covariation method described by Lika
225 et al. (2011), and the data set shown in Sup. Mat. 2. The estimation was completed using
226 the package DEBtool (following Marques et al., 2018) on the software Matlab R2020a using an
227 abj-DEB model. The parameter estimation procedures were evaluated by computing the Mean
228 Relative Errors (MRE), varying from 0, when predictions match data exactly, to infinity when
229 they do not, and the Symmetric Mean Square Errors (SMSE), varying from 0, when predictions
230 match data exactly, to 1 when they do not (<http://www.debtheory.org>) (Marques et al., 2018).

231 2.2. Individual-Based Model (IBM)

232 2.2.1. Description

233 The ODD framework (Grimm et al., 2020) was followed here for IBM description.

234 *Purpose.* The purpose of our IBM was to simulate realistic population dynamics of two species, *A.*
 235 *marina* and *A. defodiens* at one study site with known environmental conditions (here chl-a water
 236 concentration and Sea-Surface Temperature) and to infer the latitudinal heterogeneity of the two
 237 species' performances from changes in environmental forcings alone.

238 *Process overview.* The IBM accounted for different processes influencing the *Arenicola* spp. pop-
 239 ulation dynamics not included in the DEB models such as migration, density restrictions and
 240 adult/juvenile mortality (due to ageing, predation, disease or harvesting). Spawning and recruit-
 241 ment were set to happen according to the individual maturity level (obtained from the DEB model),
 242 the availability of the stage-related habitat and, in the case of spawning, favourable temperature
 243 conditions (Fig. 1). Stochasticity was introduced in the model via inter-individual variability in
 244 DEB parameters described previously.

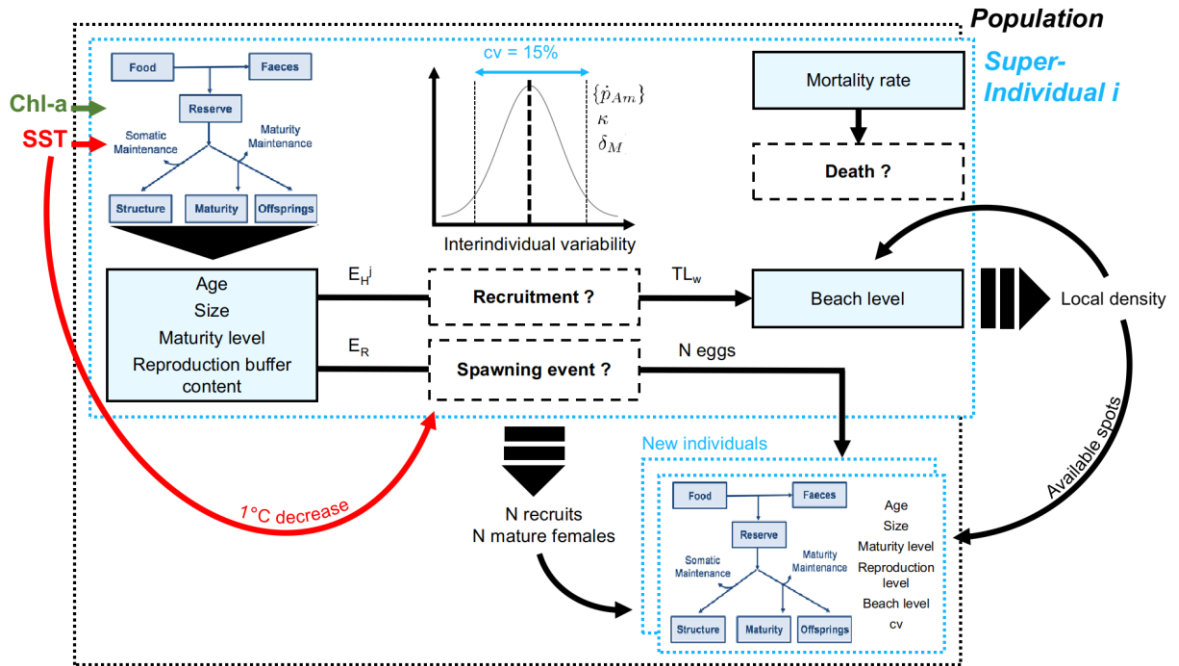


Figure 1: Representation of the different physiological, behavioural and population processes considered in the Dynamic Energy Budget Individual-Based model (DEB-IBM). Chl-a is the chlorophyll-a concentration of the seawater and SST the Sea-Surface Temperature. cv is the coefficient of variation around the normal distribution of the DEB parameters \hat{p}_{Am_i} , the maximum assimilation rate, κ , the allocation fraction to soma, and δ_M , the shape coefficient. E_H^I is the energy threshold of the maturation compartment at which metamorphosis happens. E_R is the energy content in the reproduction buffer. TL_w is the trunk length of super-individuals and N stands for number.

245 *Entities.* In order to reduce calculation times, *A. marina* and *A. defodiens* super-individuals were
 246 created. Since shore location on the beach for *A. marina* depends on its length and local density
 247 (see below) we could not define a single super-individual per cohort and instead simulated a greater

1
2
3
4
5
6
7
8
9
10
11
12
13
14
15
16
17
18
19
20
21
22
23
24
25
26
27
28
29
30
31
32
33
34
35
36
37
38
39
40
41
42
43
44
45
46
47
48
49
50
51
52
53
54
55
56
57
58
59
60
61
62
63
64
65

248 number of super-individuals accounting for a fixed number of individuals. Each super-individual
249 possessed a set of parameters, and all the individuals represented by a super-individual shared the
250 same state variable values. The number of individuals represented by a super-individual allowed
251 for low densities to occur at fine scale and was defined at the study site Wimereux (Eastern
252 English Channel, France), where each super-individual would not account for more than 1% of
253 the population. Given the potential discrepancies in density between the two species and the
254 maximum densities per shore level observed (De Cubber et al., 2018; Pires et al., 2015), one super
255 *A. marina* individual accounted for 16 individuals and one super *A. defodiens* individual accounted
256 for 4 individuals. Each super-individual possessed a set of DEB parameters and its related State
257 Variables (Table 1) were computed at each time step along with its location on the foreshore, its
258 survival and the production of new individuals (Fig. 1). The overall population dynamics was
259 considered as the sum of each individual dynamic (Fig. 1).

260 *Space.* Population dynamics were simulated on the same hypothetical shore based on the one
261 existing at Wimereux (Eastern English Channel, France), where numerous ecological studies (e.g.
262 structure of population, density, reproduction, migration...) have been carried out. Its dimensions
263 were of 1 meter large and 600 meters long (Fig. 2, see De Cubber et al., 2018, 2019 and 2020 for
264 further details). On this shore, subtidal level is under 0m of bathymetry, infralittoral level is above
265 the subtidal level up to 200m from the subtidal level limit and +2m of bathymetry, mediolittoral
266 inferior level is above the infralittoral level up to 200m from the infralittoral level limit and +4m
267 of bathymetry, and mediolittoral superior level is above the mediolittoral inferior level up to 200m
268 from the mediolittoral inferior level limit and +6m of bathymetry (constant slope, Fig. 2).

269 *Individual-based processes for A. marina.* *A. marina*'s adults spawned on the shore (see 1 in Fig 2
270 b). In order to define spawning dates for *A. marina*, we used spawning dates reported by various
271 authors at two locations (France and Scotland), and considered that spawning was a result of a
272 certain value of decreasing temperature and a certain gonado-somatic index (in this case, GSI was
273 the wet weight of gametes divided by the total wet weight of the individual) as these two parameters
274 are usually used in reproduction buffer emptying rules (Pethybridge et al., 2013; Watson, 2000).
275 The maximum number of new individuals was set according to DEB results and until recruitment,
276 larvae remained in the subtidal environment. Larval mortality was supposed to be 0.06 indiv.d⁻¹
277 (Ellien, 2004). Recruitment was set to happen at metamorphosis ($E_H = E_H^J$) (see 2 in Fig 2 b).
278 Recruits of *A. marina* settled on the high mediolittoral shore following several authors' observations
279 (Fig. 2, Sup. Mat. 1, De Cubber et al., 2018; 2020; Farke and Berghuis, 1979 a; b; Newell, 1949;
280 1948; Reise, 1985; Reise et al., 2001)). Down-shore migrations of juveniles and adults of *A. marina*
281 were simulated based on the previous study of De Cubber et al. (2020) using the relationships
282 between the length of the worms and the bathymetry of the shore level (see 3 in Fig. 2). For
283 juvenile and adult stages, survival and mortality rates were also poorly known and might vary.

284 Therefore, we considered a constant mortality rate for both adults and juveniles for *A. marina*
 285 derived from field observations (parameter estimation is described hereafter).

286 *Individual-based processes for A. defodiens*. As almost no data was available regarding environ-
 287 mental or biological triggers for *A. defodiens*' spawning events, spawning was forced each year in
 288 mid-December for this species (see 1 in Fig. 2 c).

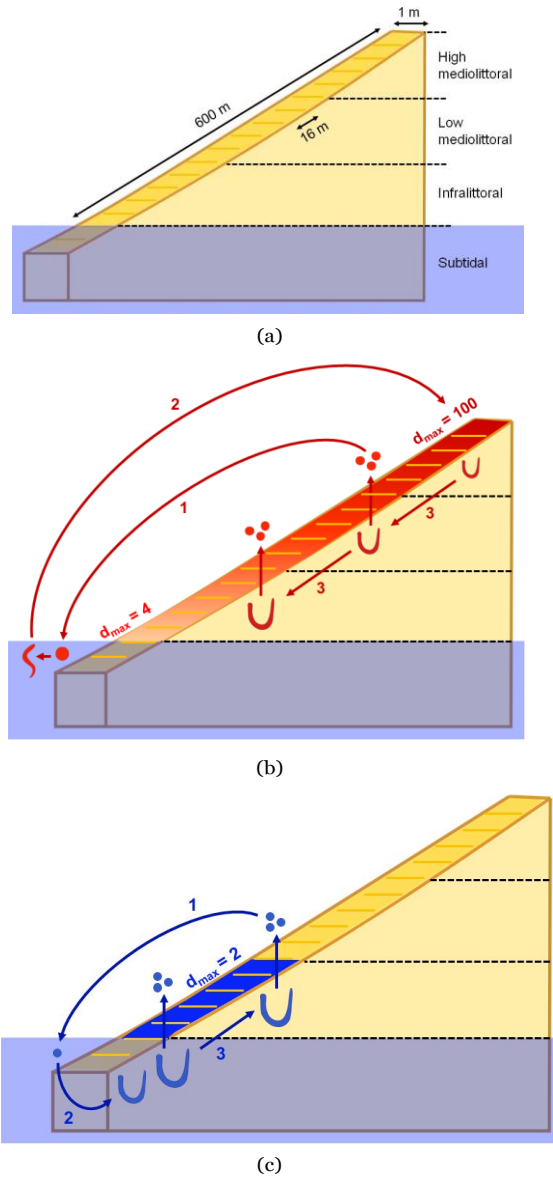


Figure 2: Simulated shore features in terms of grid definition, shore levels and shore length (a), associated uses of the shore by the different life stages and maximum density settings (d_{max} in $individuals.m^{-2}$) of (b) *A. marina* and (c) *A. defodiens*. For *A. marina*, numbers relate to (1) spawning, (2) recruitment and (3) shore migration. For *A. defodiens*, they relate to (1) spawning, (2) subtidal settlement and (3) shore colonisation at adult stage. Cells dimensions were 1 m large and 4 m long. For representation concerns, the number of cells represented is not realistic. U-shaped individuals are adults, S-shaped individual are larvae and O-shaped individuals are embryos. Cell density d is calculated as the number of individuals within each grid cell at each time step. For *A. marina*, d_{max} varies linearly along the foreshore between 100 $individuals.m^{-2}$ on the upper foreshore and 4 $individuals.m^{-2}$ on the lower foreshore. For *A. defodiens*, d_{max} (2 $individuals.m^{-2}$) is constant over the infralittoral foreshore (the species cannot colonise the mediolittoral foreshore).

1
2
3
4
5
6
7
8
9
10
11
12
13
14
15
16
17
18
19
20
21
22
23
24
25
26
27
28
29
30
31
32
33
34
35
36
37
38
39
40
41
42
43
44
45
46

289 The maximum number of new individuals was set according to DEB results and larvae remained
290 in the subtidal environment (see 2 in Fig. 2 c). Larval mortality was supposed to be $0.06 \text{ indiv. d}^{-1}$
291 (Ellien, 2004). Recruitment was set to happen at metamorphosis ($E_H = E_H^j$). Recruits of *A.*
292 *defodiens* remained in the subtidal habitat until sexual maturation ("puberty"). Adults of *A.*
293 *defodiens* reached randomly the infralittoral shore once puberty was reached ($E_H = E_H^p$), and
294 remained there until their death (see 3 in Fig. 2 c, Sup. Mat. 1) (Table 1). Since *A. defodiens* live
295 in deeper galleries and because no data was available regarding mortality rate for the species, we
296 used the same value than for *A. marina* but divided by 2.

297 *Density-dependant processes and interactions.* Density-dependent processes such as recruitment
298 have been reported for *A. marina* and might be linked to competition for food, or stability of the
299 gallery within the sediment (Reise et al., 2001; Flach and Beukema, 1994). Maximum densities
300 per shore level occupied by the two species were set according to empirical and literature data (De
301 Cubber, 2018; Pires et al., 2015) (Fig. 1). Local densities at each time step and each cell of the shore
302 grid were calculated and compared with the maximum possible density within each cell to determine
303 if new arrivals through recruitment or migration could happen in the targeted cell,(Table 1). The
304 number of new offspring produced and simulated by one female was also set according to the number
305 of available spots on recruitment grounds (all species considered) rather than according to the real
306 number of offspring produced by each female according to the DEB model. In detail, if the number
307 of offspring potentially emitted (simulated by the DEB model) surviving until metamorphosis was
308 superior to the number of available spots on recruitment grounds, the number of offspring simulated
309 was set equal to the number of available spots on recruitment grounds at this time step times 2
310 (to avoid cases where early mortality would lead to a number of recruits inferior to the number of
311 available spots on recruitment grounds), divided by the number of females spawning at the same
312 time step (Fig. 1, Table 1). Otherwise, it was set equal to number of offspring emitted simulated
313 by the DEB model. Inter-specific competition could happen when large *A. marina* individuals
314 would reach available spots on the infralittoral shore, hence limiting the number of spots available
315 for *A. defodiens* individuals.

316 *Computation and initialisation.* The DEB-IBM was run ten times at each of the 28 study sites
317 in order to account for stochastic variations in the model outputs on NetLogo 6.2.0 software
318 (<https://ccl.northwestern.edu/netlogo/>). The model was initialised with a first pool of 600 *A.*
319 *marina* super-individuals (larvae) and a first pool of 90 *A. defodiens* super-individuals (larvae)
320 allowing populations to colonise the shore and survive until the next year. Simulations were run
321 over 20 years with a daily time step (the first 10 years were run for model stabilisation and the out-
322 puts of the last 10 years were used for results analyses). Subsequent data analyses and statistical
323 analyses were performed on Matlab R2020a.

1
2
3
4
5
6
7
8
9
10
11
12
13
14
15
16
17
18
19
20
21
22
23
24
25
26
27
28
29
30
31
32
33
34
35
36
37
38
39
40
41
42
43
44
45
46
47
48
49
50
51
52
53
54
55
56
57
58
59
60
61
62
63
64
65

324 2.2.2. Parameter estimation

325 Three parameters were estimated: the GSI, the fall of temperature, both controlling the spawn-
326 ing events, and the daily mortality rate, regulating death for *A. marina* only. First, the daily
327 mortality rate, \hat{m} , was adjusted with a constant spawning period in mid-September as observed at
328 Wimereux (Wx, France, Eastern English Channel), where values from $1 \cdot 10^{-4}$ indiv.d⁻¹ to $2.5 \cdot 10^{-3}$
329 indiv.d⁻¹ were tested (Sup. Mat. 3.1), close to what was observed in the literature (Then et al.,
330 2015). The daily mortality rate was assessed on the basis of a relationship between simulated mean
331 density and mortality rate for the Wx reference site (6.5 indiv.m^{-2} , De Cubber et al., 2018). The
332 daily mortality value obtained from this model was used for all sites in this study (Sup. Mat. 1).

333 Second, the GSI and the fall of temperature were assessed by testing a decrease rate from 0 to
334 2°C in 2 weeks' time (0.25°C increment) and a GSI from 0.05 to 0.16 (0.01 increment) all together
335 (Sup. Mat. 3.2). Each couple of values were considered consistent with observations when 80% of
336 the spawning events happened between early September and early December at Wx and at East
337 Sands (St Andrews, Scotland) (De Cubber et al., 2018; Watson et al., 2000). In case further choice
338 was needed, the parameters leading to a GSI of 0.1 were used, close to previous values reported at
339 Wx (De Cubber et al., 2019).

340 2.3. Environmental data

341 Daily Sea-Surface Temperature (SST, 4 km² resolution : www.cersat.ifremer.fr) and monthly
342 chlorophyll-a concentration (chl-a, 1 km² resolution : www.hermes.acri.fr) time series were ex-
343 tracted from satellite data at 28 locations where lugworms have been described (Fig. 3 and Sup.
344 Mat. 4) over a 10 years' time period (2010-2020).

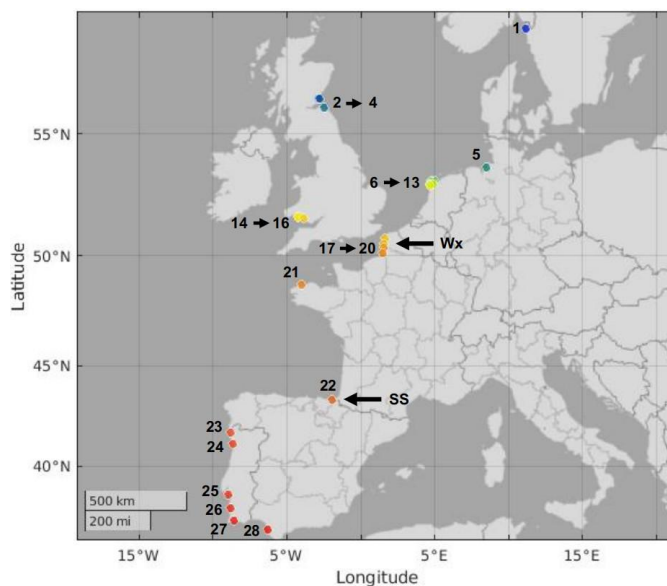


Figure 3: Studied sites (and site number) from the North East Atlantic where lugworm populations dynamics and biological traits were investigated according to local Sea-Surface Temperature and Chlorophyll-a data. Sites correspond to areas where *A. marina* and/or *A. defodiens* were described. Further details on the sites are given in Sup. Mat. 4. Sites colours are used hereafter in the results section. On black sites, environmental data were not available or their resolution was too low, and no simulations were run.

1
2
3
4
5
6
7
8
9
10
11
12
13
14
15
16
17
18
19
20
21
22
23
24
25
26
27
28
29
30
31
32
33
34
35
36
37
38
39
40
41
42
43
44
45
46
47
48
49
50
51
52
53
54
55
56
57
58
59
60
61
62
63
64
65

345 Only sites where the extracted data covered more than 30% of the time series were kept in the
346 study. In order to allow simulations to stabilise over the simulation period (which took around
347 9 to 10 years), they were performed using two cycles of 10 years. For each site, only one cell of
348 each environmental forcing map was used. When one SST data point was missing and in between
349 monthly chl-a values, interpolations were made on Matlab R2019a using the Interp1 function
350 (simple linear method used for Temperature as missing values were scarce, and Modified Akima
351 cubic Hermite interpolation used for chl-a concentration values, allowing for some undulations).

352 2.4. DEB-IBM output analyses

353 2.4.1. Model stability

354 The number of simulation runs needed was assessed according to Ritter et al. (2011). 52 runs
355 of the model were made at one studied site (Wimereux). 1000 groups of 2 to 50 runs among the
356 52 runs performed were selected with a bootstrap method. Mean of mean abundance in between
357 group sizes as well as variations in mean abundance in between groups were computed through
358 the standard deviation of means (σ) and the standard error of means (*SEM*, Equation 1). *SEM*
359 differences between group sizes N and $N - 1$ were also computed. The number of runs chosen
360 allowed *SEM* stability (Sup. Mat. 5).

$$SEM \sim \sigma \sqrt{\frac{1}{N}} \quad (1)$$

361 2.4.2. Latitudinal patterns of biological traits

362 At each site for both species, the mean abundance and biomass, the variations in abundance
363 and biomass, the total reproductive output (*TRO*), the maximum length ($L_{max, population}$), the
364 length at puberty ($L_{p, population}$), and the spawning periods were extracted from model outputs.
365 The mean abundance and biomass were the means per site over the last 9 years of the simulation.
366 The variations of mean abundance and biomass (total stock biomass, *TSB*) were the daily values
367 of abundance and biomass over the last 9 years of the simulation. *TRO* was computed as the sum
368 of the number of oocytes spawned per all simulated lugworm during the period of simulation at
369 each location. $L_{max, population}$ at death per site and per period was computed as the mean of the
370 higher 10% values of the length at death of lugworms. $L_{p, population}$ was computed as the mean
371 length at puberty of all the individuals that had been simulated at one location for one species
372 (Table 1). For the spawning periods, at each location, a Gaussian curve was fitted over the daily
373 number of lugworms spawning per Julian day (1 to 365) over the last 10 years of the simulation
374 with the Matlab R2020a function *fitdist*, after checking that each data set could be represented by
375 a standard and normal distribution with a one-sample Kolmogorov-Smirnov test (Matlab R2020a
376 function *kstest*).

377 2.4.3. Fine-scale biological traits per location

378 For two sites with contrasted model predictions (site 17: Wimereux and 22: San Sebastian,
379 see Fig. 3 and Sup. Mat. 4 and 6), the mean shore levels occupied (gravity centre) in terms of

1
2
3
4 380 biomass and abundance for each species were calculated at each time step (every day) (see Table 1),
5 381 Y being the biomass or the abundance of the species at the considered site, x the bathymetry, Y_x
6 382 the biomass or abundance at bathymetry x , and G_Y the center of gravity of Y (mean bathymetry).
7 383 The size (0.5 cm trunk length classes) distribution on the shore for each species at each time step
8 384 was also recorded at these sites.

10 385 2.4.4. Influence of chlorophyll-*a* concentration and temperature

11 386 The same model outputs were computed using the environmental variables' time series showing
12 387 the highest, lowest and median mean values over the whole time period. Biological trait values cor-
13 388 responding to those 9 conditions (3 chl-*a* conditions x 3 SST conditions) were compared calculating
14 389 the index $r = \frac{\text{trait value} - \text{mintrait value}}{\text{maxtrait value} - \text{mintrait value}}$ varying from 0 to 1.

20 390 3. Results

21 391 3.1. Environmental variables

22 392 The mean values of SST and concentration of chl-*a* per site over the period 2010-2020 highlighted
23 393 some contrasted latitudinal gradients, where the highest SST values were found beneath latitude
24 394 45° N whilst the highest chl-*a* values were found above latitude 50° N (Fig. 4 a and b, Sup. Mat.
25 395 7.1 and 7.2). There were some exceptions in the chl-*a* gradient, with values sometimes higher close
26 396 to some south estuaries (North Coast of Portugal) (Fig. 4 b, Sup. Mat. 7.1). Each site displayed
27 397 the same seasonal SST pattern with highest SST values in summer and lowest SST values in winter
28 398 (Fig. 4 c). Chl-*a* also displayed some seasonal pattern with pikes between March and September
29 399 but some variations in-between sites could be observed (Fig. 4 d).

30 400 3.2. Model parameters

31 401 3.2.1. Calibration of DEB parameters of *A. defodiens*

32 402 The parameter estimation of the abj-DEB model for *A. defodiens* provided a MRE of 0.19 and
33 403 SMSE of 0.27 (Sup. Mat. 2). All data used for model calibration are freely available within the
34 404 Add-my-Pet collection (https://bio.vu.nl/thb/deb/deblab/add_my_pet/index.html) and in Sup.
35 405 Mat. 2. DEB parameters of *A. defodiens* (and *A. marina*) are provided in Table 2.

36 406 3.2.2. Calibration of DEB-IBM parameters

37 407 Mortality m of juveniles and adults of *A. marina* at Wimereux was estimated at $8.16 \cdot 10^{-4}$
38 408 indiv.d⁻¹ (Table 2, Sup. Mat 3.1). The values of decrease of SST over two weeks (T_{spawn}) and
39 409 GSI threshold ($GSI_{trigger}$) simulating more than 80% of the lugworms spawning within the main
40 410 observed spawning period (end of August to beginning of December) were respectively of 1°C per
41 411 14 days and 0.1 (Table 2, Sup. Mat. 3.2).

1
2
3
4
5
6
7
8
9
10
11
12
13
14
15
16
17
18
19
20
21
22
23
24
25
26
27
28
29
30
31
32
33
34
35
36
37
38
39
40
41
42
43
44
45
46
47
48
49
50
51
52
53

412 3.3. Latitudinal population responses to environmental parameters

413 3.3.1. Population abundance and biomass

414 After simulation over the 28 studied sites, *A. marina*'s population density (abundance.m⁻²) and
415 *TSB* appeared the highest above the latitude 49° N and in Northern Portugal, and the lowest in
416 Southern Spain and Portugal as well as in France below latitude 49° N (Figs. 5 a, b), but not
417 leading to any populations' crashes (Figs. 6 a, c).

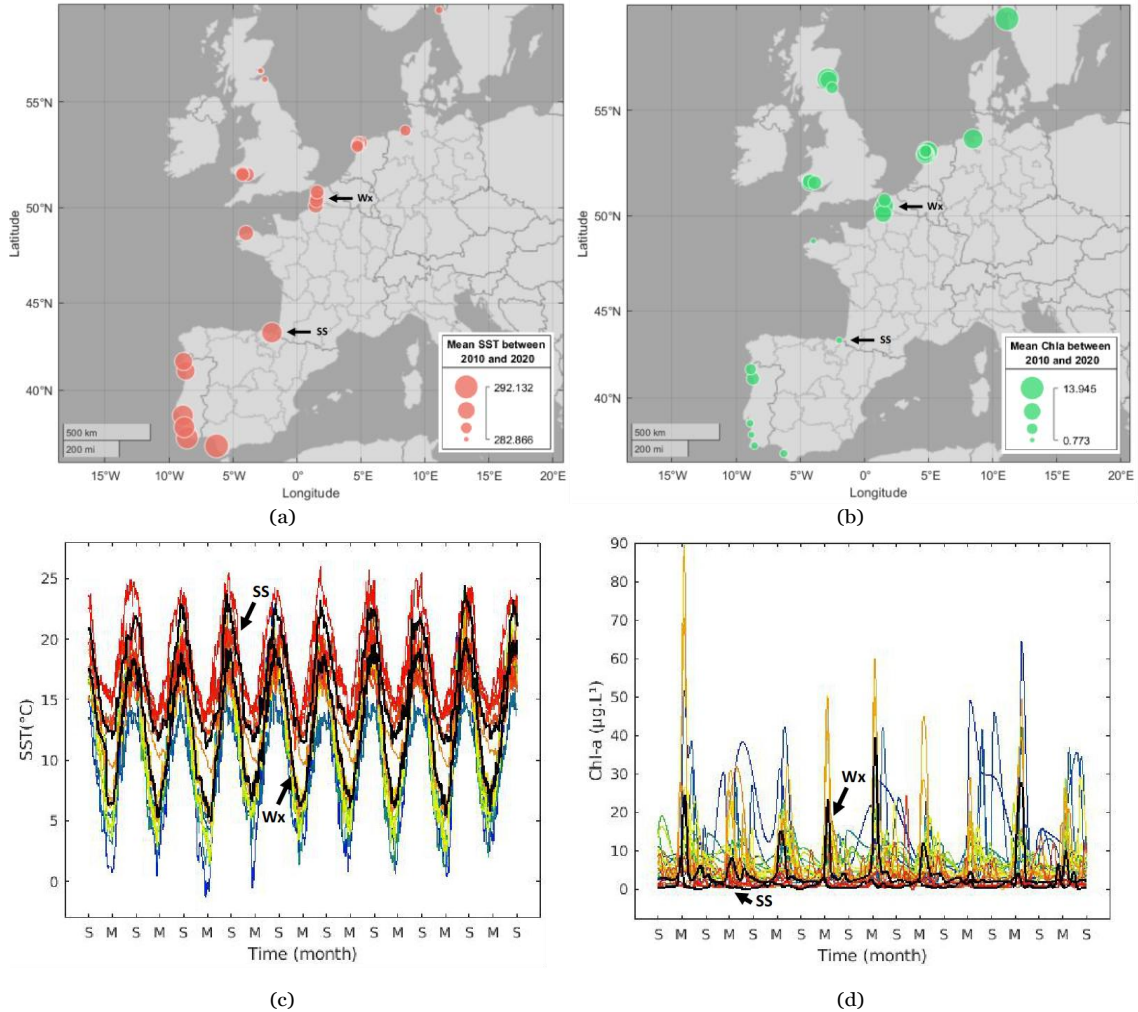


Figure 4: (a) Mean Sea-Surface Temperature (*SST*, K) and (b) Chlorophyll-a concentration (*chl a*, µg.L⁻¹) between 2010 and 2020 at each of the 28 sites where lugworms occurrences were recorded. (c) Associated *SST* variations and (d) *Chl-a* variations at each site between 2010 and 2020 (S stands for September and M for March), from higher latitudes in blue to lower latitudes in red. Variations in both environmental variables are represented in black at Wimereux (Wx) and San Sebastian (SS). Both environmental forcings were obtained from satellite data (respectively extracted from www.cersat.ifremer.fr at a 4 km² resolution and from www.hermes.acri.fr at a 1 km² resolution).

-2

418 For *A. defodiens*'s population, density (abundance.m⁻²) and *TSB* appeared the highest above
419 the latitude 45° N and in Northern Portugal, and the lowest in Southern Spain, Portugal and in
420 France below latitude 45° N (Figs. 5 c, d), where simulations led to a population crash (Figs.
421 6 b, d). Population crashes either happened from the beginning of the simulation, in this case
422 initialized individuals did not survive, either at other times of the simulation when overall density

423 was high some time before (Sup. Mat. 8). Overall, population crashes seemed associated to low
 424 levels of chl-a associated to high SST (Sup. Mat. 8).

Table 2: Summary of the primary and some auxiliary parameters of the abj-Dynamic Energy Budget models as well as the Individual-Based model for *A. marina* and *A. defodiens*. TTR stands for Temperature Tolerance Range, MT for Maturation Threshold.

Parameter	Symbol	<i>A. marina</i> Value	<i>A. defodiens</i> Value	Unit
Dynamic Energy Budget parameters				
Reference temperature ¹	T_{ref}	293.15 ^b	293.15 ^a	K
Fraction of food energy fixed in reservio ¹	κ_X	0.80 ^b	0.80 ^a	-
half-saturation coefficient for chl-a	X_K	5.00 ^b	5.00 ^b	$\mu\text{g.L}^{-1}$
Arrhenius temperature	T_A	4014 ^b	4568 ^a	K
Arrhenius temperature under the TTR	T_{AL}	69080 ^b	-	K
Arrhenius temperature over the TTR	T_{AH}	82380 ^b	-	K
TTR's lower boundary	T_L	272.8 ^b	-	K
TTR's higher boundary	T_H	297.7 ^b	-	K
Energy conductancio ²	ψ	9.77 10 ^{-03b}	0.0207 ^a	cm.d^{-1}
Allocation fraction to soma	κ	0.90 ^b	0.83 ^a	-
Reproduction fraction fixed in eggs ¹	κ_R	0.95 ^b	0.95 ^a	-
Volume specific costs of structure	r_{EGS}	4123 ^b	4209 ^a	$J.\text{cm}^{-3}$
MT for the trochophore larva	E_H^{tr}	1.11 10 ^{-03b}	8.69 10 ^{-04a}	J
MT for birth	E_H^b	1.77 10 ^{-03b}	1.03 10 ^{-03a}	J
MT for metamorphosis	E_H^j	3.19 ^b	3.52 ^a	J
MT for puberty	E_H^p	104.10 ^b	12.32 ^a	J
Acceleration rate ³	s_M	12.13 ^b	14.92 ^a	-
Maximum assimilation rate ²	$t\beta_{AmU}$	10.99 ^b	8.89 ^a	$J.\text{cm}^{-2}.\text{d}^{-1}$
Specific somatic maintenance rate	$[\beta_M]$	15.6 ^b	28.87 ^a	$J.\text{cm}^{-3}.\text{d}^{-1}$
Maturity maintenance rate ¹	$\hat{\kappa}_J$	2.00 10 ^{-03b}	2.00 10 ^{-03a}	d^{-1}
Shape parameter until birth	δ_{Me}	0.66 ^b	0.66 ^b	-
Shape parameter after metamorphosis	δ_M	0.231 ^b	0.1601 ^a	d^{-1}
Specific density of wet structure ¹	d_V	1 ^b	1 ^a	g.cm^{-3}
Specific density of wet reserve ¹	d_E	1 ^b	1 ^a	g.cm^{-3}
Specific density of dry reserve ¹	d_{Ed}	0.16 ^b	0.16 ^a	g.cm^{-3}
Specific chemical potential of dry reserve ¹	μ_{Ed}	550000 ^b	550000 ^a	$J.\text{Cmol}^{-1}$
Molar weight of dry reserve ¹	w_{Ed}	23.9 ^b	23.9 ^a	g.Cmol^{-1}
Inter-individual variability coefficient	c_v	15 ^a	15 ^a	%
Individual-Based Model parameters				
Gonado-Somatic Index spawning threshold	$GS_{trigger}$	10 ^a	-	%
Temperature decrease spawning threshold	ΔSST_{14}	1 ^a	-	$K.14\text{d}^{-1}$
Mortality rate	\hat{m}	8 . 10 ^{-04a}	4 . 10 ^{-04a}	indiv.d^{-1}
Maximum local density - high mediolittoral	d^{high}	100 ^c	-	indiv.m^{-2}
Maximum local density - low infralittoral	d^{low}	4 ^c	-	indiv.m^{-2}
Maximum local density - subtidal	d^{sub}	4 ^c	2 ^c	indiv.m^{-2}
Larval survival rate	\hat{s}	0.94 ^d	0.94 ^d	indiv.d^{-1}
Female ratio	$ratio_f$	0.5	0.5	-

¹ Fixed parameters. The values were taken from the generalized animal (Kooijman, 2010).

² These are the values at birth

³ s_M is given for a scaled functional response of 1 after metamorphosis

References associated to the parameter values: ^aThis study, ^bDe Cubber et al. (2020), ^cDe Cubber et al. (2018) and ^dEllien et al. (2004)

425 For *A. marina*, yearly variations in abundance and TSB could be observed at most sites where
 426 abundances exceeded 1000 individuals due to recruitment (Fig. 6 a), whilst they were much more
 427 reduced for *A. defodiens* (Fig. 6 b). Indeed, for the latter species, individuals could remain on the

1
2
3
4
5
6
7
8
9
10
11
12
13
14
15
16
17
18
19
20
21
22
23
24
25
26
27
28
29
30
31
32
33
34
35
36
37
38
39
40
41
42
43
44
45
46
47
48
49
50
51
52
53
54
55
56
57
58
59
60
61
62
63
64
65

428 subtidal environment and colonise the infralittoral foreshore as soon as densities allowed it (empty
429 spots).

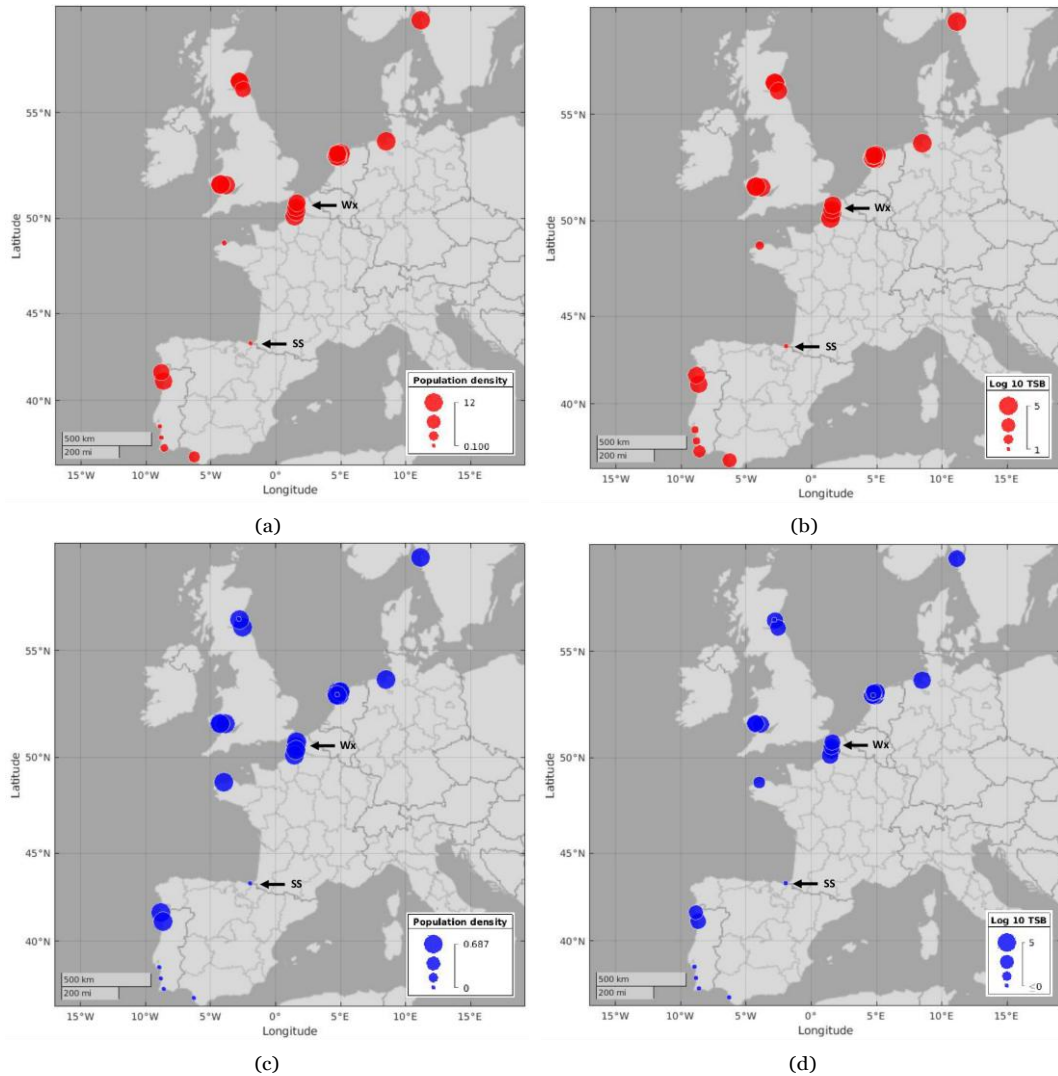


Figure 5: Projections of mean population density (individuals.m⁻², left) and log 10 total stock biomass TSB (juveniles + adults) (g, right) of *A. marina* (top, red) and *A. defodiens* (bottom, blue) at the 28 studied locations between 2010 and 2020 of the Dynamic Energy Budget Individual Based Model developed in this study.

430 3.3.2. Total reproductive output

431 *TRO* overall displayed the same latitudinal patterns than abundance and *TSB* for both species,
432 with up to 4 orders of magnitude of difference between the highest and the lowest values for *A.*
433 *marina* and 10 (as some populations crashed and could not produce offspring, see sites 26 and 29)
434 for *A. defodiens* (Fig. 7).

435 3.3.3. Maximum length and length at puberty

436 The mean $L_{p,population}$ varied between 2.5 (San Sebastian, Spain) and 3 cm (northern sites) for
437 *A. marina* and between 0 (Roscoff, France) and 1.6 cm (northern sites) for *A. defodiens* (Figs. 8
438 a and c).

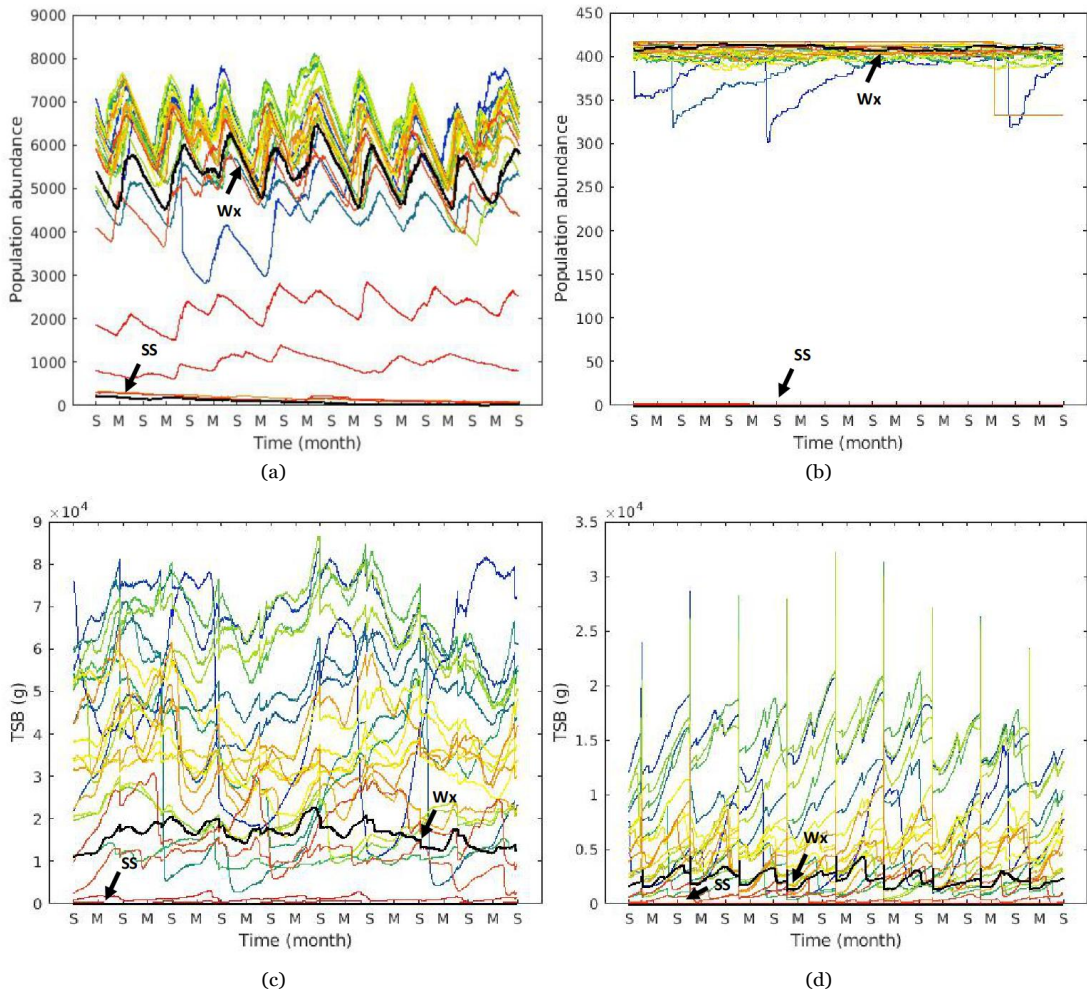


Figure 6: Projection of the evolution of *abundance* (number of individuals on the foreshore) (a, b) and Total Stock Biomass (*TSB*, g) (c, d) at the 28 studied locations for *A. marina* (left, a, c) and *A. defodiens* (right, b, d) from 2010 to 2020 (S stands for September and M for March). Coldest colors stand for sites of the highest latitudes and warmest colors for the sites of the lowest latitudes (see Fig. 3).

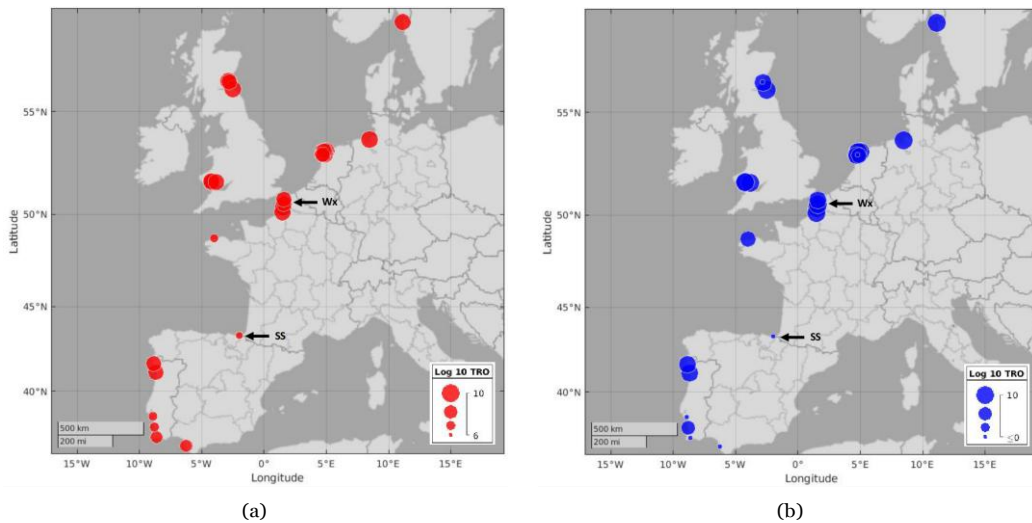
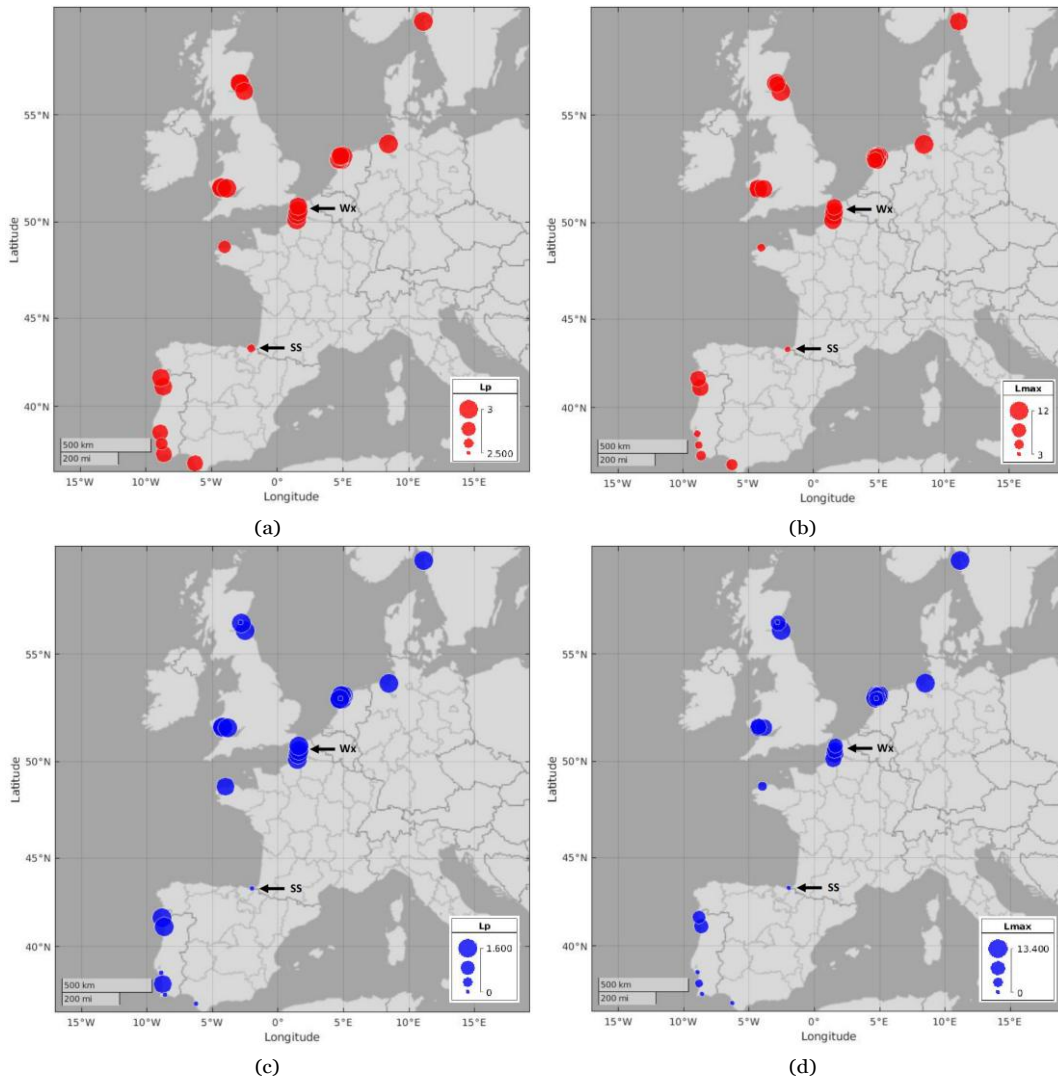


Figure 7: Projections of total reproductive output (*TRO*) of *A. marina* (left, red) and *A. defodiens* (right, blue) at the 28 studied locations between 2010 and 2020 of the Dynamic Energy Budget Individual Based Model.

439 $L_{max,population}$ followed a similar pattern, varying between 3.3 and 12 cm for *A. marina*, with
 440 minimum and maximum at the same locations, and between 0 (San Sebastian, Spain, where pop-
 441 ulations crashed) and 13.4 cm for *A. defodiens* (also at northern sites) (Figs. 8 b and d). Both
 442 biological traits displayed the same latitudinal patterns described for abundance, *TSB* and *TRO*,
 443 the minimal values of $L_{p,population}$ being obtained where individuals reached the lowest sizes.

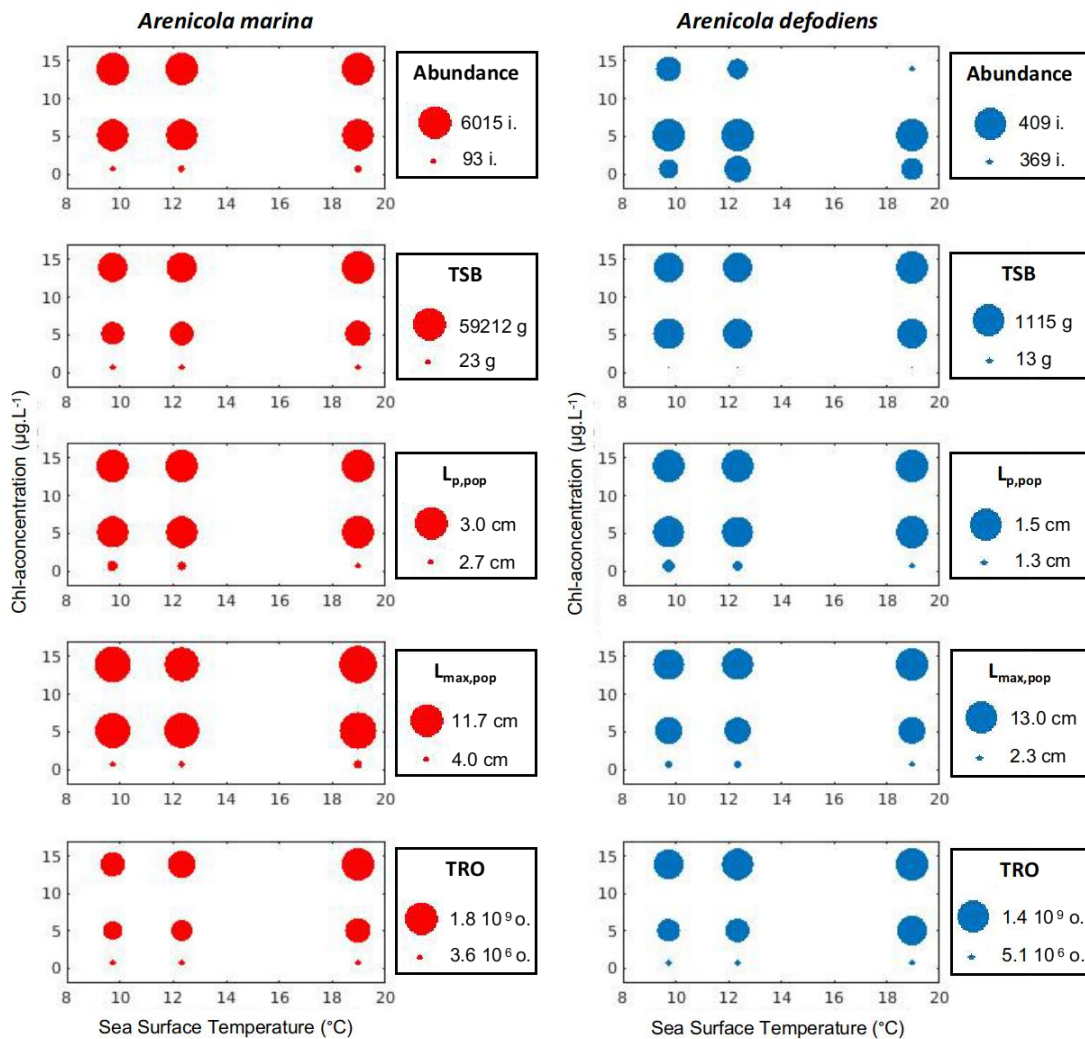


47 Figure 8: Projections of mean length at puberty $L_{p,population}$ (cm, left) and mean length of the 10% longer
 48 individuals $L_{max,population}$ (cm, right) of *A. marina* (top, red) and *A. defodiens* (bottom, blue) at the 28 studied
 49 locations between 2010 and 2020 of the Dynamic Energy Budget Individual Based Model developed in this study.

51 3.4. Influence of chlorophyll-a concentration and Sea-Surface Temperature

52 Population responses of *A. marina* and *A. defodiens* in terms of the five targeted biological
 53 traits (*abundance*, *TSB*, $L_{p,pop}$, $L_{max,pop}$ and *TRO*) to different scenarios of mean SST and chl-a
 54 were compared. The relative outputs (maximum diameter corresponding to the higher value and
 55 minimum diameter to the lower value of the biological trait) followed the same pattern for all
 56 biological trait except *abundance*: biological trait values increased with increasing chl-a levels and,
 57 to a much lesser extent, with increasing SST (the latter pattern was mainly observable for *TRO*).
 58
 59
 60
 61
 62
 63
 64
 65

451 Overall, chl-a had more influence than SST on all biological traits for both species (Fig 9). However,
 452 populations' responses to chl-a and SST in terms of abundance were different between species:
 453 populations of *A. marina* reached high abundance when chl-a $\approx 5 \mu\text{g.L}^{-1}$, whilst populations of *A.*
 454 *defodiens* did not display clear pattern for abundance with neither chl-a concentration nor SST. As
 455 abundance values for *A. defodiens* varied between 334 to 416 individuals (same level of magnitude)
 456 when those for *A. marina* varied between 34 to 6408 individuals, low abundance of *A. defodiens*
 457 did not impact greatly *TSB*. The fact that *TSB* and other biological traits followed the same
 458 trends for *A. defodiens* and for *A. marina* seems to point out that the abundance pattern observed
 459 for *A. defodiens* is linked to the interplay between environmental parameters and competition for
 460 space with large individuals of *A. marina* on the infralittoral foreshore (that manage to grow and
 461 reach this shore level only in the best environmental conditions).



58 Figure 9: Relative values of mean abundance, mean total stock biomass (*TSB*), mean length at puberty ($L_{p,pop}$ or
 59 $L_{p,population}$), maximum length ($L_{max,pop}$ or $L_{max,population}$), and total reproductive output (*TRO*) of populations
 60 simulated with the 9 scenarios of chlorophyll-a concentration and Sea-Surface Temperature for *A. marina* (red, left),
 61 and *A. defodiens* (blue, right).

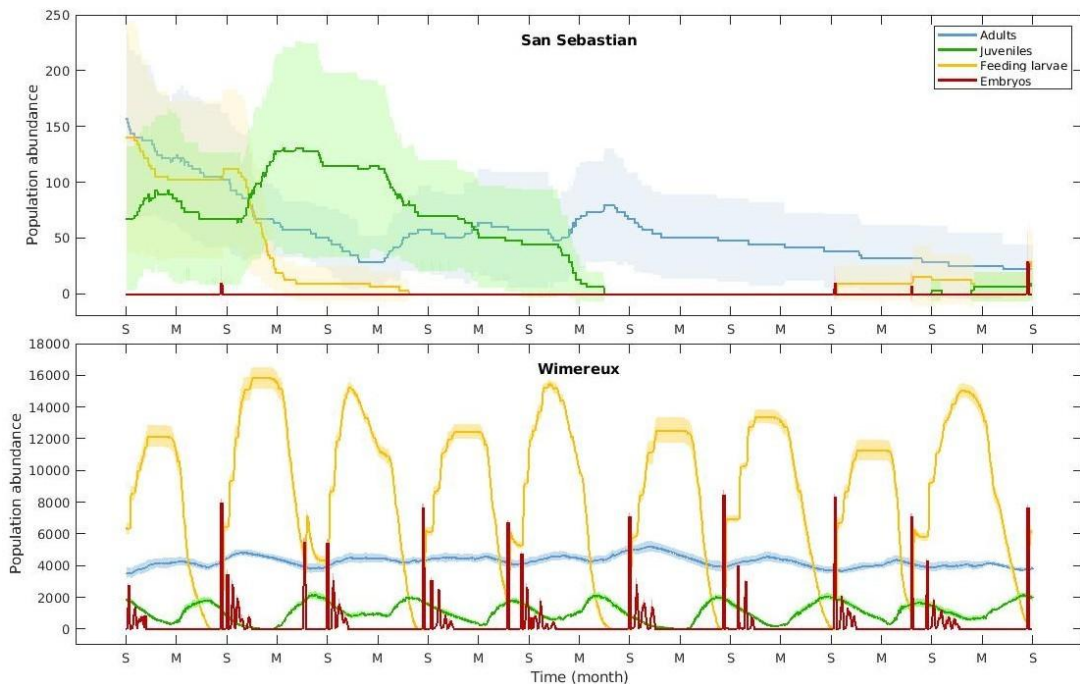
1
2
3
4
5
6
7
8
9
10
11
12
13
14
15
16
17
18
19
20
21
22
23
24
25
26
27
28
29
30
31
32
33
34
35
36
37
38
39
40
41
42
43
44
45
46
47
48
49
50
51
52
53
54
55
56
57
58
59
60
61
62
63
64
65

462 3.5. Fine-scale underlying mechanisms

463 Different patterns in populations' biological traits were observed such as at Wimereux (Wx)
464 and San Sebastian (SS) (Fig. 3). The corresponding population dynamics were investigated more
465 closely in terms of life-stage dynamics, shore colonisation and inter-individual variability.

466 3.5.1. Life-stage dynamics of *A. marina*

467 For *A. marina*, the typical pattern of yearly spawning (embryo/trochophore larva pikes) around
468 September and recruitment (juvenile waves) in spring documented at Wx were accurately repro-
469 duced by the DEB-IBM, with the adult population remaining quite stable around 4000 individuals
470 yearly renewed every year by the arrival of new individuals (Fig. 10). However, at SS, spawning
471 events did not occur every year and the adult population appeared extremely low and variable with
472 150 down to 20 individuals. There, only a very small, if not negligible, portion of the population
473 managed to spawn and population decreased (Fig. 10).



46 Figure 10: DEB-IBM simulated abundance of embryos (dark red), feeding larvae (yellow), juveniles (green) and
47 adults (blue) according to time (S stands for September and M for March) of two populations of *A. marina*: San
48 Sebastian (Spain, top) and Wimereux (France, bottom). Lines correspond to the mean value obtained from the 10
49 simulations, shaded areas upper and lower limit correspond to more or less one standard deviation.

50
51
52
53
54
55
56
57
58
59
60
61
62
63
64
65

474 3.5.2. Shore colonisation

475 The simulated mean bathymetry occupied on the foreshore by *A. marina* displayed different
476 patterns between Wimereux (Wx) and San Sebastian (SS) as well (Fig 11). At Wx, the number of
477 lugworms was simulated higher on the mediolittoral superior foreshore once a year (corresponding
478 to the typical pattern for recruitment) and then individuals migrated down to the lower infralittoral
479 shore, the mean bathymetry occupied at this point being also influenced by the presence of larvae
480 in the subtidal environment (Fig. 11). At SS, the fine scale distribution pattern was quite different

1
2
3
4
5
6
7
8
9
10
11
12
13
14
15
16
17
18
19
20
21
22
23
24
25
26
27
28
29
30
31
32
33
34
35
36
37
38
39
40
41
42
43
44
45
46
47
48
49
50
51
52
53
54
55
56
57
58
59
60
61
62
63
64
65

481 with no clear recruitment pattern as previously described in Fig. 10. There, a high proportion
482 of lugworms in the simulated population occupied the higher shore for the first four years as
483 juveniles were more numerous than adults at this point (see Fig. 10). When adults started to be
484 in the majority, their lower shore level remained higher than at Wimereux linked to a lower mean
485 maximum size, as shore migration is linked to length for this species (see Fig. 8b).

486 At Wx, the mean shore levels of *A. defodiens* remained difficult to analyse because of the
487 non-negligible subtidal pool of individuals for this species (Fig. 11). However, it appeared that
488 both species occurred on the infralittoral shore at least part of the year (Fig. 11). Inter-specific
489 interactions were therefore further studied.

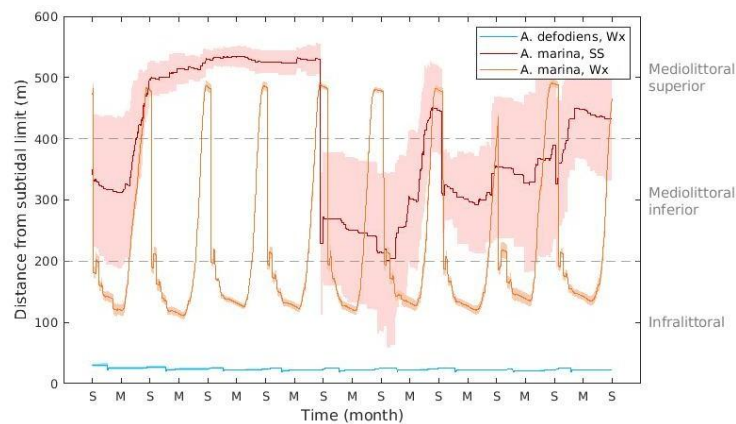


Figure 11: Mean shore level (expressed in m from subtidal limit) simulated in terms of abundance for *A. marina* and *A. defodiens* obtained at Wimereux (orange, blue) and San Sebastian (dark orange).

490 3.5.3. Density-dependant recruitment of *A. marina*

491 For *A. marina*, the number of juveniles (recruits of the year) was related to the number adults
492 on the foreshore (Fig. 12).

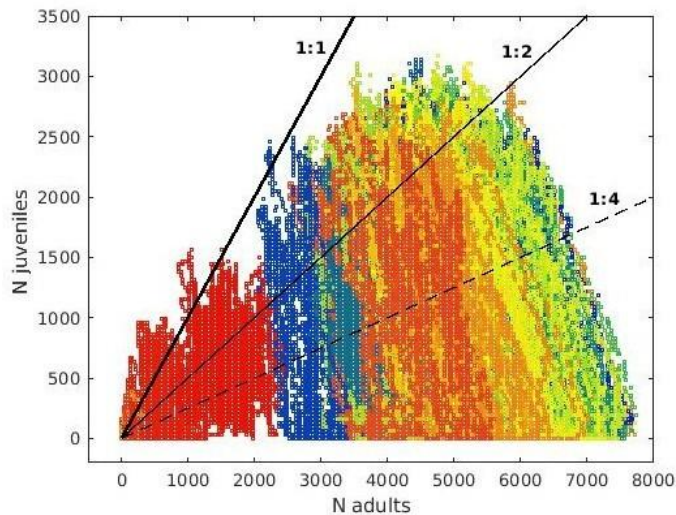


Figure 12: Number of juveniles according to the number of adults on the shore (b) at the 28 sites (coldest colors stand for sites of the highest latitudes and warmest colors for the sites of the lowest latitudes) at each time step.

At southern sites with overall low number of adults ($d'1000$ individuals), the proportion of juveniles reached values superior to 50% as adult lugworms did not survive a really long time there (Fig. 12). Overall, the maximum number of juveniles increased with the number of adults until adult populations levels around 5000 individuals. At this point, their numbers could reach more than 3000 individuals (Fig. 12). Indeed, the more abundant is the species, the higher is its maximum length, hence the lower its level on the shore is, leaving more space for juveniles to recruit. For populations above 5000 adults, the maximum number of juveniles and their proportion decreased revealing density-limiting recruitment for these populations (Fig. 12).

3.5.4. Inter-specific interactions

Inter-specific interactions were explored focusing on the relations between mean simulated abundances of *A. defodiens* and mean simulated abundances and minimum shore level occupied by *A. marina* (Fig. 13).

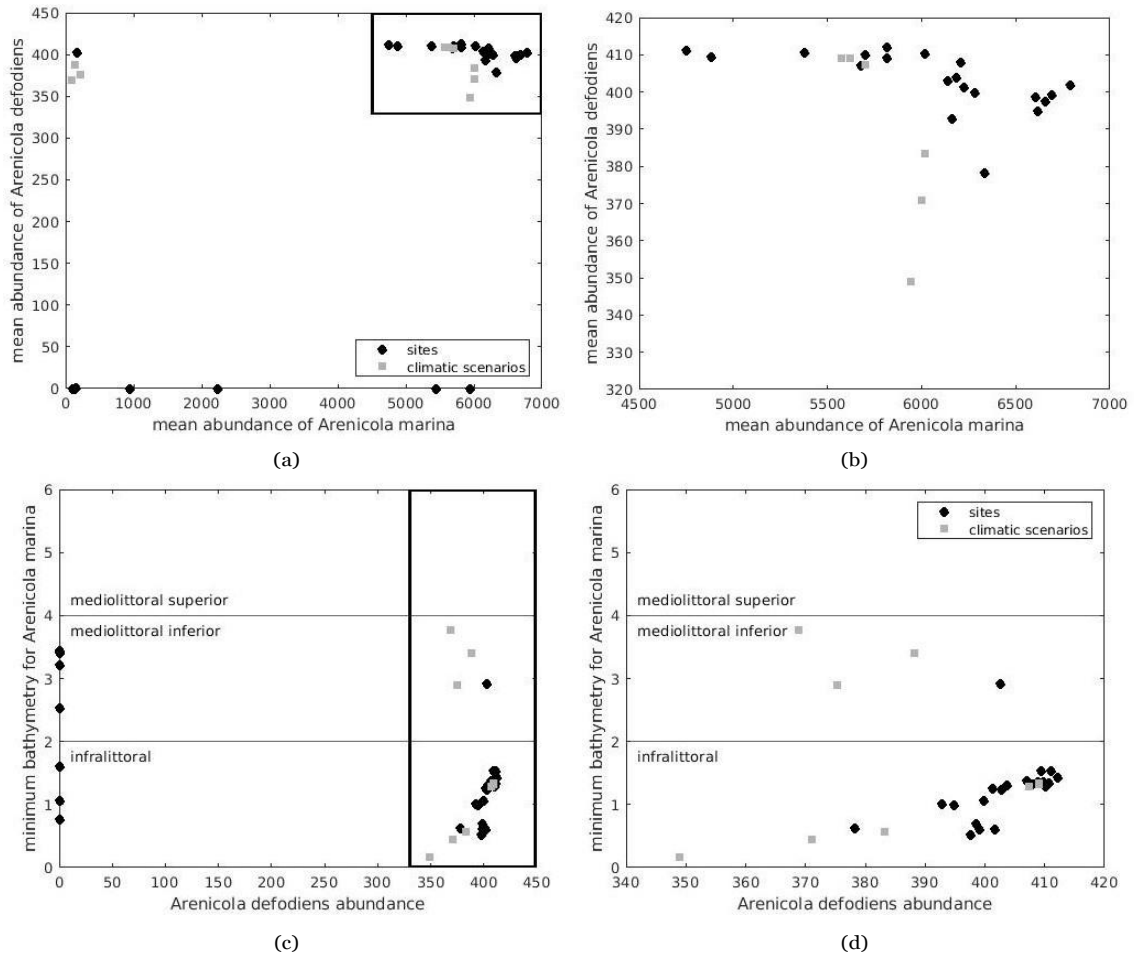


Figure 13: Mean abundance of *A. defodiens* according to the mean abundance of *A. marina* (a, b) and minimum bathymetry (m) of *A. marina* according to the abundance of *A. defodiens* (c, d) simulated at the 28 studied sites (black dots) and for the 9 climatic scenarios (grey squares). Boxes in Figs a and c represent the axes of Figs b and d. Horizontal lines in Figs c and d are the limit of the foreshore levels.

It appeared that, when environmental conditions allowed it (boxes on Figs. 13 a and c focus

1
2
3
4
5
6
7
8
9
10
11
12
13
14
15
16
17
18
19
20
21
22
23
24
25
26
27
28
29
30
31
32
33
34
35
36
37
38
39
40
41
42
43
44
45
46
47
48
49
50
51
52
53
54
55
56
57
58
59
60
61
62
63
64
65

506 on the cases where species thrive), and when *A. marina* was in sympatry with *A. defodiens* (e.g.
507 reached the infralittoral level as shown on Figs. 11 and 13 d), high abundances of *A. marina* (over
508 6000 individuals) on potentially higher surface of the infralittoral shore (with lower bathymetry
509 level reached) slightly negatively impacted the abundance of *A. defodiens* (Fig 13).

510 3.5.5. Size distribution and size at puberty

511 Inter-individual variability allowed for individuals of the same age to reach different sizes,
512 leading to the presence of cohorts of varying sizes (Fig. 14). It also lead to varying sizes at puberty
513 for each individuals in between populations and within one population (Fig. 15).

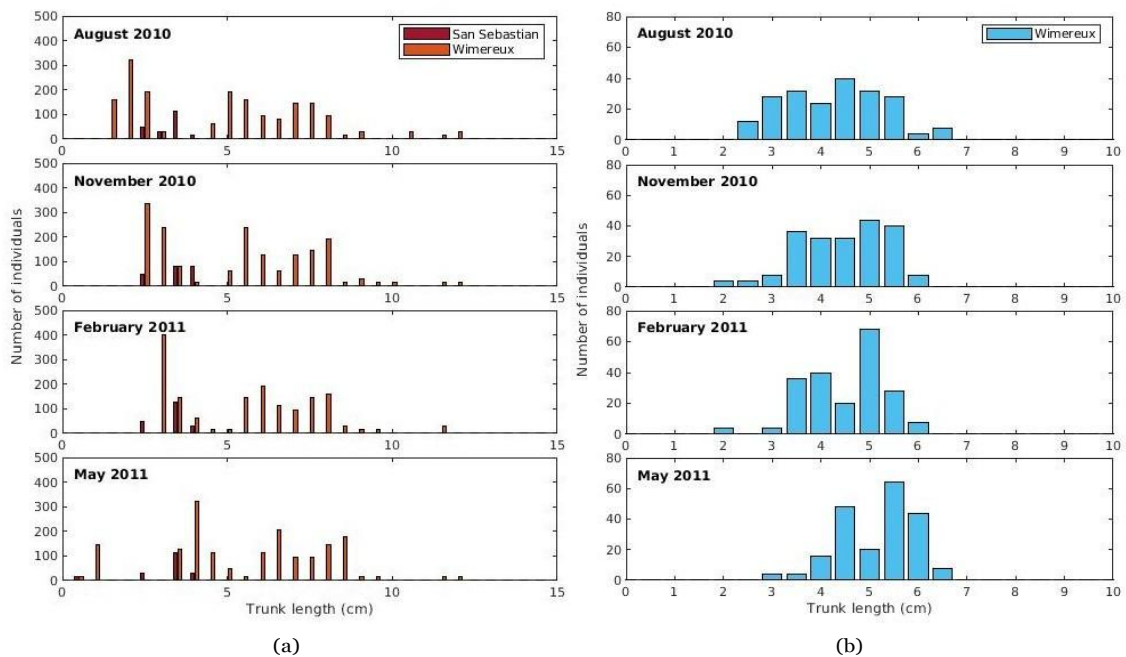


Figure 14: Size distribution of the *A. marina*'s (a) and *A. defodiens*' (b) populations simulated by the DEB-IBM model in San Sebastian (dark red) and Wimereux (light orange and light blue) in August 2010, November 2010, February 2011 and May 2011.

514 For *A. marina*, size distributions at Wx and at SS appeared different, with individuals reaching
515 up to 12 cm (trunk length) at Wx and less than 5 cm at SS (Fig. 14 a). Age cohorts at SS were
516 extremely difficult to distinguish probably linked to a low growth rate, whilst age cohorts for ages
517 0+ (under 1 year old, 2 ~ 0.5 cm in August 2010) and 1+ (under 2 years old, 3 to 4 ~ 0.5 cm
518 between November 2010 and May 2011) could clearly be identified at Wx, recruitment (e.g. the
519 arrival of smaller individuals) happening between April-May and August (Fig. 14 a). Puberty was
520 reached between 2.8 and 3 cm at Wx and between 2.1 and 2.9 cm at SS (Fig. 15).

521 For *A. defodiens*, sizes at Wx ranged from 2 to 7 cm in trunk length (Fig. 14 b). Age cohorts
522 could not be clearly identified but it appeared that shore colonisation by young adults happened
523 rather during autumn and winter, smaller individuals being present only in November and February
524 (Fig. 14 b). At this site, puberty was reached between 1.4 and 1.5 cm (Fig. 15).

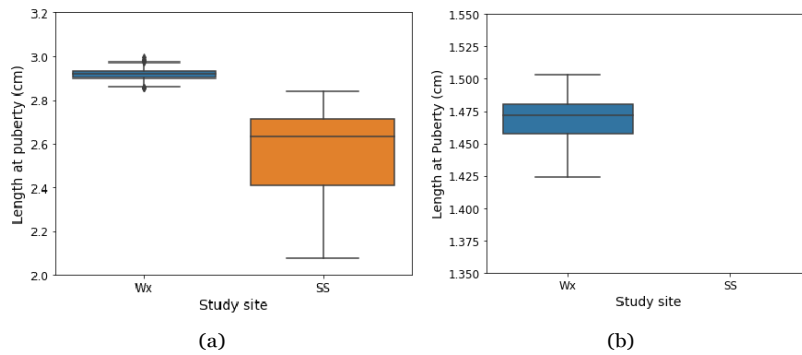


Figure 15: Boxplot distributions in length at puberty of *A. marina* (a) and *A. defodiens* (b) populations simulated by the DEB-IBM model in San Sebastian (SS, orange) and Wimereux (Wx, blue).

4. Discussion

In August 2023, only 47 research articles out of the 5138 DEB-related research articles accessible in Web of Science (www.webofscience.com) dealt with DEB-IBMs, allowing the upscaling from individual to population levels. Among these, upscaling was achieved through generation of new individuals based on reproduction and through mortality. Combining these processes with variability of model parameters, and mobility and habitat preferences appeared even less common. In this study, the population dynamics, biological traits and shore distribution of two engineer polychaete species were mechanistically modelled in the North-East Atlantic along a latitudinal gradient using a newly developed fine-scale spatially-explicit DEB-IBM considering all these processes. The model allowed both comparison of mean biological traits among sites over a large range of environmental conditions and fine scale exploration of the on-shore mechanisms behind these macroscopic discrepancies. This kind of approach appears essential to provide a better understanding of marine populations, and potentially further community and ecosystem responses to small-scale (such as local shore fisheries) and large-scale (changing environmental conditions) human impact on the environment.

4.1. Main results

4.1.1. Empirical validation of the DEB-IBM

Our model's predictions of latitudinal distribution of population biological traits, of the impact of environmental forcings and of on-shore population processes and dynamics appeared in accordance with the majority of the body of literature existing about both species and was considered as an empirical qualitative validation of the DEB-IBM.

Predictions of the environmental scenarios. While environmental parameters displayed opposite trends, with overall northern regions displaying lower SST and higher chl-a concentration compared to southern regions displaying higher SST and lower chl-a concentration, the lower value of one did not compensate a higher value of the other. Indeed, SST latitudinal changes between sites did not impact greatly populations dynamics while higher concentrations of chl-a induced at the

1
2
3
4
5
6
7
8
9
10
11
12
13
14
15
16
17
18
19
20
21
22
23
24
25
26
27
28
29
30
31
32
33
34
35
36
37
38
39
40
41
42
43
44
45
46
47
48
49
50
51
52
53
54
55
56
57
58
59
60
61
62
63
64
65

551 same time higher maximum length, reproductive output and abundance. The idea that currently
552 temperature is generally not a limiting factor for *A. marina* is in accordance with first De Cubber
553 et al. (2020), who showed that shore migrations of lugworms are more likely to be linked with food
554 concentration rather than temperature constraints, and second, with Wethey and Woodin (2022),
555 who represented *A. marina*'s current area of distribution following extreme temperatures along
556 most of the European Atlantic coasts.

557 *Predictions of the latitudinal responses.* *A. marina*'s observations have been made from Portugal
558 to Norway (Cadman and Nelson-Smith, 1993; De Cubber et al., 2018; Luttikhuisen and Dekker,
559 2010; Pires et al., 2015; Watson and Bentley, 1997) and are in accordance with our predictions
560 of the species' latitudinal distribution. Predictions of *A. defodiens*'s latitudinal distribution also
561 coincide with observations of the species made in Wales, the Eastern English Channel, the North
562 Sea as well as in one lagoon of Portugal (Cadman and Nelson-Smith, 1993; De Cubber et al., 2018;
563 Luttikhuisen and Dekker, 2010; Pires et al., 2015; Watson and Bentley, 1997). As it seems that
564 population crashes for the species are linked to low levels of chl-a associated to high values of SST,
565 the species might have thrived in Portugal, where it has been introduced, due to the high values
566 of chl-a observed within the lagoon (close to sites 23 and 24 studied here).

567 *Population-level processes.* The DEB-IBM developed here considers most of the reviewed physio-
568 logical (growth, reproduction and development) and behavioural mechanisms (density-dependant
569 recruitment and foreshore migration and length-dependent foreshore migration) involved in *A. ma-*
570 *rina* and *A. defodiens*' populations dynamics and their relation to environmental parameters (De
571 Cubber et al., 2018; 2019; 2020; Flach and Beukema, 1994; Reise et al., 2001; Watson et al, 2000).
572 Some processes yet not fully described such as metabolic processes for *A. defodiens*, inter-individual
573 variability in metabolic processes for both species, universal spawning thresholds for *A. marina*
574 and mortality rates were added either based on novel experimental data (for *A. defodiens*), or on
575 the literature, using available data. At a local scale, our results reproduce the trends obtained on
576 the field in previous studies in terms of spawning and recruitment periods, zonation on the shore
577 levels, shore migration and size distribution for *A. marina* (De Cubber et al., 2018;2020; Reise et
578 al., 2001; Watson, 2000). Indeed, in our DEB-IBM, the reproduction period happens from late
579 summer to mid autumn for *A. marina* as recorded by several authors (De Cubber et al., 2018;
580 Watson et al, 2000), the recruitment period mostly occurs in late spring with a smoother pike (De
581 Cubber et al., 2020; Reise et al., 2001), and an effect of adult shore density was shown on re-
582 cruitment, as described by Flach and Beukema (1994). Recruitment indeed happens on the higher
583 shore, where juveniles migrate down the shore while growing as previously described (De Cubber
584 et al., 2020; Reise et al., 2001). Finally, simulated *A. marina*'s population size structure displayed
585 similar patterns than those previously recorded at Wx in terms of mean size at age (around 4 cm
586 for 1 year-old individuals in May, see De Cubber et al., 2020) and of coefficient of variation around

1
2 587 the mean size (10 to 20%, see De Cubber et al., 2020).
3

4 588 4.1.2. Underlying mechanisms 5

6 589 *Density-dependant dynamics.* Inter and intra-specific density-dependant interactions (competition)
7 590 emerged from our model model properties. They could be observed only in the most favourable
8 591 environmental conditions. Intra-specific density dependant recruitment for *A. marina* has been
9 592 documented in the past in the Wadden Sea (Reise et al., 2001; Flach and Beukema, 1994), whilst
10 593 competition between *A. defodiens* and *A. marina*, although predicted by our model, has not yet
11 594 been studied to our knowledge. Indeed, mean population abundances of *A. defodiens* appear partly
12 595 dependent on the abundance of *A. marina* at the lower shore under favourable environmental
13 596 conditions. Such competition should be further studied to validate this aspect in our model, or to
14 597 improve it in future versions. Different reasons could explain this competition, among which the
15 598 competition for space (the smaller galleries being destroyed by larger individuals), for food and for
16 599 oxygen, or a combination of these. The fact that species live or not in sympatry (Cadman, 1997)
17 600 seems related to their ability to survive and thrive in a given environment. Low chl-a concentrations
18 601 will be related to the absence of *A. defodiens* and the presence of rare *A. marina* individuals, while
19 602 high chl-a concentrations will be related to the presence of both *A. defodiens* and *A. marina* on
20 603 the lower shore.
21

22 604 *Maturity size selection.* Puberty was reached for larger sizes under favourable environmental con-
23 605 ditions, and for lower sizes with a higher size variability at sites with less favourable environmental
24 606 conditions, thus selecting individuals with a higher κ parameter in the first case and a smaller
25 607 one in the second case. This could mean either that a selection of individuals reaching maturity
26 608 early happens at sites with poor environmental conditions, or that under favourable environmental
27 609 conditions, meaning high abundances, and thus higher intra-specific competition, these individuals
28 610 do not manage to thrive and die early. The exact mechanism for this selection should be further
29 611 studied in the future. In all cases if the site produces the majority of larvae that will recruit there,
30 612 this could lead to differentiated populations displaying slightly different DEB parameters (such as
31 613 a smaller κ).
32

33 614 *Tipping points.* Two types of tipping points, that "lead to abrupt and possibly irreversible shifts
34 615 between alternative ecosystem states" (Dakos et al., 2019) could be detected and will be worth
35 616 studying in the future. First, the one type leading to *A. defodiens*' population crash, that seemed
36 617 linked to the temporal evolution of environmental forcings and their combination. Unless popula-
37 618 tions did not survive from the beginning, they appeared quite unpredictable in some cases where
38 619 the population abundance was high and decreased abruptly. Second, the tipping point leading
39 620 from a *A. marina*' population that displays the typical recruitment-spawning pattern and where
40 621 the population is renewed and stable through time to a population with a really low number of
41 622 individuals, and rare spawning and recruitment event. Although related to poor chl-a conditions,
42
43
44
45
46
47
48
49
50
51
52
53
54
55
56
57
58
59
60

1
2
3
4
5
6
7
8
9
10
11
12
13
14
15
16
17
18
19
20
21
22
23
24
25
26
27
28
29
30
31
32
33
34
35
36
37
38
39
40
41
42
43
44
45
46
47
48
49
50
51
52
53
54
55
56
57
58
59
60
61
62
63
64
65

623 this latter tipping point might also occur in cases where mortality is high due to harvesting (Olive,
624 1993), and where recruitment is low due to poor quality of the surrounding subtidal temporary
625 habitats of larvae (De Cubber et al., 2018).

626 4.2. Limitations

627 4.2.1. Knowledge on *A. defodiens*' biology

628 The combination of the estimation of the energy maturation threshold for puberty, E_H^p , which
629 is approximately 10 times lower for *A. defodiens* than for *A. marina*, and of a lower κ seems in
630 accordance with biological observations of the two species (Table 2). Indeed, it is likely that *A.*
631 *defodiens* invests indeed more energy in reproduction than *A. marina* with for instance 4000 oocytes
632 per day for a black lugworm of 10 cm (this study) against 1000 oocytes per day for the lugworm
633 *A. marina* of the same size (De Cubber et al. 2020), or reaches puberty (which is equivalent to
634 age at first maturity in DEB vocabulary) earlier, as observations of gamete production were made
635 in *A. defodiens* individuals much smaller (1.5 cm TLw; Gaudron unpublished) than what has been
636 observed for *A. marina* (2.5 cm TLw; De Cubber et al., 2018, Table 2). However, maximum trunk
637 length for *A. defodiens* might be higher as we based this value in the calibration process on data
638 collected at sites 17, 18 ,19 and 20 (Sup. Mat. 4 and 6) where the species does not reach the
639 highest maximum length value (Sup. Mat. 6)

640 4.2.2. Pelagic and benthic subtidal part of the life cycle

641 Little is known regarding the subtidal part of the life cycle of both species. As a consequence,
642 we did not consider larval dispersal and survival, nor the presence or the absence of temporary
643 subtidal settlement habitats for larvae, which might impact recruitment success (Lewin, 1986; De
644 Cubber et al., 2018; 2019). This would require additional data as well as a better understanding of
645 these aspects on the lugworm's lifecycle and on potential subtidal habitats. However this could be
646 implemented in the future through the coupling of the DEB-IBM with biophysical model combining
647 a model of physical circulation (MARS-3D model developed within the English Channel, see Ayata
648 et al., 2009) and a larval transport model based on biological parameters such as the date of
649 spawning, the number of emitted larvae, and the pelagic larval dispersal duration (e.g. time
650 spent in the water column) (Failletaz, 2015). DEB models could provide the biological parameters
651 needed to implement the larval dispersal model. Such a model could then allow to understand
652 the populations' connectivity in the area (identifying the possible sources and sinks of propagules
653 for example) and thus give valuable information for the conservation of the species. Populations
654 genetics through the study of the gene fluxes could be combined with this approach (Hedgecock
655 et al., 2007; Wright 1931). As an example, as abundances at some sites declined due to a lack
656 of self recruitment in the current study, it would be interesting to study whether these sites can
657 constantly be 'refilled' by individuals coming from other locations.

1
2
3
4
5
6
7
8
9
10
11
12
13
14
15
16
17
18
19
20
21
22
23
24
25
26
27
28
29
30
31
32
33
34
35
36
37
38
39
40
41
42
43
44
45
46
47
48
49
50
51
52
53
54
55
56
57
58
59
60
61
62
63
64
65

658 4.2.3. Regional adaptations

659 In our study, the DEB parameters of the two species do not vary geographically and the changes
660 in the populations' simulated traits are due to differences in the environmental scenarios considered
661 along the latitudinal gradient. Other DEB studies along environmental gradients have tested the
662 possibility of variations in some DEB parameters across biogeographic regions. For example, Huret
663 et al. (2018) did a regional calibration of one parameter (the maximum assimilation rate) to get
664 better fit of growth trajectories and this may suggest a genetic adaptation. However, these authors
665 acknowledge that an effect of food availability in quantity and quality could be not completely
666 discarded. Further, a covariation with some other DEB parameters can be reasonably expected.
667 Some clues seem to point out that genetic adaptation might occur for some populations of *A.*
668 *marina* as well. Indeed, Schröder et al. (2009) studied the digging activity and the respiration
669 rate for a range of temperatures (0°C to 22°C) of individuals of the species originated from three
670 different regions (Atlantic, North Sea and White Sea) and showed that individuals from different
671 regions did not display the same digging response to temperature. This would involve a change
672 in other DEB parameters (e.g. the specific somatic maintenance rate, the temperature-specific
673 parameters). Adjustments of some or all DEB parameters in-between regions could be investigated
674 further to sub-populations of the species rather than to the whole data set but this will require
675 collection of genetic data and population dynamics at the same spatial scales.

676 4.2.4. Predators and competitors

677 The estimation of the IBM mortality parameter used in this study (Table 2) could also be
678 improved as it has only been fitted for one site among the 28 investigated and it does not dissociate
679 death linked to ageing, predation, competition with other species or by harvesting pressure. As
680 our main objective was first to assess the impact of environmental variables solely on populations'
681 dynamics, and since we do not extrapolate results in terms of differences in mortality among sites,
682 we believe that this should not impact our results interpretation beyond reason. However, in
683 further studies, depending on the objectives that are aimed at, this aspect should be improved, as
684 predation can lead to varying levels of mortality depending on the predator's density (Hastings,
685 2013), possibly leading to varying mortality rates among sites and according to time. Indeed,
686 changes in predators' populations such as the sole (flat fish, De Vlas, 1979) are already reported
687 (Van de Wolfshaar et al., 2021). Then et al. (2015) recommended to use the formula $\hat{m} = 4.899 \cdot t_{max}^{-0.916}$
688 to estimate fish mortality with \hat{m} the natural mortality rate (year⁻¹) and t_{max} the
689 maximum age (year). This leads to a daily mortality rate of 0.0026 d⁻¹ for *A. marina* considering
690 $t_{max} = 6$ years (De Cubber et al., 2020), which is 3.25 times higher than what has been estimated
691 in this study (Table 2). This could be linked to phylogenetic (invertebrate vs fish) and lifestyle
692 (mainly hidden in the sediment vs open water swimming) differences between species. Competition
693 between lugworms and other species such as the eelgrass *Zostera noltii* or tube building polychaetes
694 such as *Lanice conchilega* have already been reported by several authors (Kosche, 2007; Volkenborn

1
2 695 and Reise, 2007) and this could indeed impact their population dynamics.

3 4 696 4.2.5. *Environmental variables*

5
6 697 SST and chl-a values were extracted from 1 grid cell of respectively 4 and 1 km² only at sites
7 698 where the species presence have been recorded. It could be interesting to compare our 1 cell
8
9 699 environmental forcings to to the average of 9 cells to test our environmental data's robustness,
10
11 700 although it would mean losing resolution. Other sites along the coast could also be considered in
12
13 701 future studies. Of course, SST is different from sediment temperature, especially on the higher
14
15 702 mediolittoral shore that remains emerged longer, and is used here as a proxy of the temperature
16
17 703 experienced by lugworms (De Cubber et al., 2020). However, these differences were not found to
18
19 704 impact greatly *A. marina*'s performances in terms of size and weight under current environmental
20
21 705 conditions (De Cubber et al., 2020). Chl-a is also non homogeneous at the scale of the shore as
22
23 706 well and is anyway a proxy of much more complex feeding mechanisms, but was found to be the
24
25 707 best proxy available for the species (Chennu et al., 2015; De Cubber et al., 2020). Overall, as finer
26
27 708 resolution observations at such a large scale with good quality data are not available elsewhere
28
29 709 to our knowledge, we believe that the differences of mean values and their temporal variations in
30
31 710 between sites give good ideas of latitudinal differences in between populations.

32 33 711 4.2.6. *Model validation and sensitivity analysis*

34
35 712 Quantitative validation for simulations made at Wx was not performed. However, all parame-
36
37 713 ters of the model were calibrated at this site based on a large and diverse data set obtained from
38
39 714 previous studies (De Cubber et al., 2018; 2019; 2020) and from extra experiments performed in
40
41 715 this study (see respiration experiment for *A. defodiens*). At this site, the population dynamics
42
43 716 simulated display the typical size distribution, migration (down-shore), recruitment (recruitment
44
45 717 period and recruits location on the shore) and reproduction (spawning period) patterns described
46
47 718 for the species by a number of authors (among which, De Cubber et al., 2018; 2019; 2020; Flach and
48
49 719 Beukema, 1994; Reise et al., 2001; Watson et al, 2000). Overall, we consider that these compar-
50
51 720 isons are qualitative validation of our model. To validate the model quantitatively at this site and
52
53 721 use it for management, new independent field sampling and laboratory work should be performed
54
55 722 to test its reproducibility. Besides, as the idea of this study is rather a comparison of the model's
56
57 723 behaviour in between contrasted environmental conditions than a very accurate site-specific pre-
58
59 724 diction on population traits, we believe that our results are still interesting and overall reliable. In
60
61 725 the prospect of using this model as a tool for management, a sensitivity analysis on the model's
62
63 726 parameters should also be implemented (Matyja, 2023).

64 65 727 4.3. *Model prospects*

66 67 728 4.3.1. *Fisheries*

68
69 729 In order to prevent the two species over-exploitation (Blake, 1979; Olive, 1993; De Cubber et
70
71 730 al., 2018), potentially leading to changes in size and age structure, abundance and distribution
72
73 731 of local populations, several authors have emphasised the need for managing polychaete species

1
2
3
4
5
6
7
8
9
10
11
12
13
14
15
16
17
18
19
20
21
22
23
24
25
26
27
28
29
30
31
32
33
34
35
36
37
38
39
40
41
42
43
44
45
46
47
48
49
50
51
52
53
54
55
56
57
58
59
60
61
62
63
64
65

732 (Watson et al., 2017; Xenarios, 2018). These management measures aim at limiting the overall
733 mortality, or the mortality of specific individuals in the population, based on its features (FAO,
734 2012). Such measures have been implemented in some areas, generally consisting in licensing for
735 commercial harvesters and in maximum daily catches for recreational fishermen, with in rare cases
736 (UK) local management strategies adapted to the stakes of the area (Cabral et al., 2019). The DEB-
737 IBM developed in this study could be used by conservation managers as a tool to explore several
738 management scenarios after validation procedure is performed. This could be done by adding a
739 distinction between the fishery-related mortality rate from other mortality types, and potentially
740 spatialising this new mortality rate and/or making it relative to the individuals size. For
741 example, a size limit impact on the population structure and the TRO (depending on if the size
742 limit exceeds the length at puberty or not) could be tested, as well as the impact of closing an area
743 (the entire shore or only the higher shore as suggested by De Cubber et al., 2018) to fisheries (with a
744 fisheries-related mortality set to zero in the considered area) on the overall population's dynamics.
745 Other management scenarios such as a closing season, the implementation of quotas, licenses or tool
746 restrictions could also be explored.

747 4.3.2. *Climate change and heat waves*

748 Climate change can affect the distribution and population dynamics of marine organisms (Kear-
749 ney et al., 2009; Thomas and Bacher, 2018). The Intergovernmental Panel on Climate Change
750 predicted a warming of Sea-Surface Temperature of 1 to almost 5 °C by 2100 (IPCC, 2021). In
751 this context, the DEB-IBM implemented in this study constitutes a powerful tool for predicting
752 lugworms' responses to climate change in terms of populations dynamics, biological traits by using
753 the projections in terms of SST and chl-a provided by the IPCC. However, due to the cascade of
754 impacts that occur at the land–ocean interface, biogeochemical and hydrological models still strug-
755 gle to provide accurate projections in terms of future time series for global coastal chl-a (Raimonet
756 et al., 2018).

757 Although high temperatures did not appear in this study a major issue for lugworms' survival in
758 comparison to low chl-a concentrations, marine heatwaves are likely to intensify in the next decades
759 and have already been identified as a challenge for lugworms' species (Wethey and Woodin, 2022).
760 We believe this issue could be addressed in our DEB-IBM considering the effect of oxygen content
761 of the sediment on lugworm density and shore migration. Indeed, in this study, IBM parameters
762 related to density (maximum local densities at different levels of the foreshore) were defined non-
763 mechanistically according to what was reported in the literature (Table 2, De Cubber et al., 2018).
764 An alternative method would be to consider the maximum carrying capacity of the shore in terms
765 of the oxygen content within the sediment. Indeed, lugworms can remain within emerged sediments
766 for periods exceeding 6 hours (Schöttler, 1989) leading to depletion of the surrounding oxygen or
767 food that keep being consumed by individuals. When SST increases, the dissolved oxygen decreases
768 (Aminot and Kerouel, 2004), leading to a potential decrease in lugworms density if thermal changes

1
2
3
4
5
6
7
8
9
10
11
12
13
14
15
16
17
18
19
20
21
22
23
24
25
26
27
28
29
30
31
32
33
34
35
36
37
38
39
40
41
42
43
44
45
46
47
48
49
50
51
52
53
54
55
56
57
58
59
60
61
62
63
64
65

769 are gradual, or to an increase in mortality if changes are sudden. In this case, the development of
770 a DEB model accounting for low activity levels at emersion and high activity levels at immersion
771 could be considered.

772 4.3.3. Bioturbation and impact on communities

773 Bioturbation by lugworms contributes to limit the evolution of sandy sediments to muddy
774 sediments (Volkenborn et al., 2007). Indeed, in some areas, layers of 17 to 40 cm of the whole
775 shores's sediment can be reworked annually by lugworms, depending on the size of lugworms, their
776 density, and the period of the year (temperature and food effects on metabolism) (Cadée, 1976).
777 The decline of lugworms' populations predicted by Wethey and Woodin (2022) in southern areas
778 would thus lead to new bio-physical features of these shores. Given the mechanistic properties
779 of our DEB-IBM, such decline in bioturbation could be quantified finely by adding a relation be-
780 tween lugworms size/weight and sand reworking volume according to temperature and food level
781 obtained from laboratory experiments. Such knowledge could also give insights on the possible
782 evolution of the whole associated benthic-pelagic community in a climate change context in areas
783 where lugworms will be extending or decreasing. As an example, *A. marina* has been shown to im-
784 pact negatively populations of *Zostera noltii* (Kosche, 2007) and to influence the local community
785 compositions (Donadi et al., 2015). Its observed expansion in southern areas (Pires et al., 2015)
786 might lead to shifts in the communities there. Indeed, Volkenborn and Reise (2007) showed signif-
787 icant differences in polychaete functional group composition in lugworm exclusion plots compared
788 to control and ambient plots.

789 Apart from these prospects, the mechanistic nature of our DEB-IBM makes it easily adaptable
790 to new questions from scientists and managers that might arise in the next decades. Besides,
791 despite its complexity, the construction of the model around biological processes can make it
792 understandable at least from a conceptual view to non-modelers such as conservation managers
793 and could become a valuable tool in the next years to study the *A. marina* and *A. defodiens*
794 population dynamics in a variety of situations.

795 **Acknowledgements**

796 We would like to thank L. Denis for the use of the system to carry the respiration experiments,
797 and H. Loisel for his advice on our work. We are grateful to Europe (FEDER), the state and the
798 Region Hauts-de-France for funding the experimental set up and field work, and the salaries of
799 T. Lancelot (research assistant) and L. De Cubber (Post-doctoral fellowship) through the CPER
800 MARCO 2015–2020.

801 **References**

802 Aminot, A., Kerouel, R., 2004. Hydrologie des écosystèmes marins; paramètres et analy-
803 ses,628 Ifremer. ed.

- 1
2
3
4
5
6
7
8
9
10
11
12
13
14
15
16
17
18
19
20
21
22
23
24
25
26
27
28
29
30
31
32
33
34
35
36
37
38
39
40
41
42
43
44
45
46
47
48
49
50
51
52
53
54
55
56
57
58
59
60
61
62
63
64
65
- 804 Ayata, S.-D., Ellien, C., Dumas, F., Dubois, S., Thiébaud, É., 2009. Modelling larval dis-
805 persal and settlement of the reef-building polychaete *Sabellaria alveolata*: Role of hydroclimatic
806 processes on the sustainability of biogenic reefs. *Cont. Shelf Res.* 29(13), 1605–1623.
807 <https://doi.org/10.1016/j.csr.2009.05.002>
- 808 Bacher, C., Gangnery, A., 2006. Use of dynamic energy budget and individual based models
809 to simulate the dynamics of cultivated oyster populations. *J. Sea Res.* 56, 140–155.
- 810 Batabyal, A.A., 1996. On some aspects of the management of a stochastically developing
811 forest. *Ecol. Model.* 89: 67–72.
- 812 Beaudouin, R., Dias, V., Bonzom, J. M., Péry, A., 2012. Individual-based model of *Chironomus riparius*
813 population dynamics over several generations to explore adaptation following
814 exposure to uranium-spiked sediments. *Ecotoxicology*, 21(4), 1225–1239. <https://doi.org/10.1007/s10646-012-0877-4>
815
- 816 Blake, R.W., 1979. Exploitation of a natural population of *Arenicola marina* (L.) from the
817 North-East Coast of England. *J. Appl. Ecol.* 16, 663–670. <https://doi.org/10.2307/2402843>
- 818 Cabral, S., Alves, A., Nuno, C., Pedro, F. E. C., Erica, S., João, C., Luís, C. D. F.,
819 Paula, C., João, C.-C., David, P., Ana, P., José Lino, C., 2019. Polychaete annelids as
820 live bait in Portugal: harvesting activity in estuarine systems. *Ocean Coast. Manag.*
821 <https://doi.org/10.3389/conf.fmars.2016.04.00111>
- 822 Cadée, G. C. 1976. Sediment reworking by *Arenicola marina* on tidal flats in the Dutch
823 Wadden Sea. *Netherlands J. Sea Res.* 10(4), 440–460.
- 824 Cadman, P.S., Nelson-Smith, A., 1993. A new species of lugworm: *Arenicola defodiens* sp.
825 nov. *mar. biol. Ass. U.K.* 73, 213–223. <https://doi.org/10.1017/S0025315400032744>
- 826 Cadman, P.S., 1997. Distribution of two species of lugworm (*Arenicola*) (Annelida: Poly-
827 chaeta) in South Wales. *J. Mar. Biol. Assoc. U.K.* 77, 389–398. <https://doi.org/10.1017/S0025315400071745>
828
- 829 Caswell, H., 2001. *Matrix Population Models: Construction, Analysis and Interpretation.*
830 Sunderland, Massachusetts: Sinauer Associates, Inc. Publishers, 2nd edition, 722.
- 831 Chennu, A., Volkenborn, N., De Beer, D., Wethey, D.S., Woodin, S.A., Polerecky, L., 2015.
832 Effects of Bioadvection by *Arenicola marina* on Microphytobenthos in Permeable Sediments.
833 *PLoS One* 10, e0134236.
- 834 Clarke, L.J., Hughes, K.M., Esteves, L.S., Herbert, R.J.H., Stillman, R.A., 2017. Intertidal
835 invertebrate harvesting: a meta-analysis of impacts and recovery in an important waterbird
836 prey resource. *Mar. Ecol. Prog. Ser.* 584, 229–244. <https://doi.org/10.3354/meps12349>

- 1
2
3
4
5
6
7
8
9
10
11
12
13
14
15
16
17
18
19
20
21
22
23
24
25
26
27
28
29
30
31
32
33
34
35
36
37
38
39
40
41
42
43
44
45
46
47
48
49
50
51
52
53
54
55
56
57
58
59
60
61
62
63
64
65
- 837 Coulson, T., 2012. Integral projections models, their construction and use in posing hypothe-
838 ses in ecology. *Oikos* 121: 1337–1350.
- 839 Dakos, V., Matthews, B., Hendry, A. P., Levine, J., Loeuille, N., Norberg, J., Nosil, P.,
840 Scheffer, M., De Meester, L., 2019. Ecosystem tipping points in an evolving world. *Nat.*
841 *Ecol. Evol.*, 3(3), 355–362. <https://doi.org/10.1038/s41559-019-0797-2>
- 842 David, V., Joachim, S., Tebby, C., Porcher, J. M., Beaudouin, R., 2019. Modelling population
843 dynamics in mesocosms using an individual-based model coupled to a bioenergetics model.
844 *Ecol. Model.*, 398(March), 55–66. <https://doi.org/10.1016/j.ecolmodel.2019.02.008>
- 845 Davis, A. J., Jenkinson, L. S., Lawton, J. H., Shorrocks, B., Wood, S., 1998. Making mistakes
846 when predicting shifts in species range in response to global warming. *Nature* 391, 783–786.
847 <https://doi.org/10.1038/35842>
- 848 De Angelis, D. L., Grimm, V., 2014. Individual-based models in ecology after four decades.
849 *F1000 Prime Reports*, 6–39. <https://doi.org/10.12703/P6-39>
- 850 De Cubber, L., Lefebvre, S., Fisseau, C., Cornille, V., Gaudron, S.M., 2018. Linking life-
851 history traits, spatial distribution and abundance of two species of lugworms to bait collection:
852 A case study for sustainable management plan. *Mar. Environ. Res.* [https://doi.org/10.1016](https://doi.org/10.1016/j.marenvres.2018.07.009)
853 [/j.marenvres.2018.07.009](https://doi.org/10.1016/j.marenvres.2018.07.009)
- 854 De Cubber, L., Lefebvre, S., Lancelot, T., Denis, L., Gaudron, S. M., 2019. Annelid poly-
855 chaetes experience metabolic acceleration as other Lophotrochozoans: Inferences on the life
856 cycle of *Arenicola marina* with a Dynamic Energy Budget model. *Ecol. Model.* 410, 108773.
857 <https://doi.org/10.1016/j.ecolmodel.2019.108773>
- 858 De Cubber, L., Lefebvre, S., Lancelot, T., Duong, G., Gaudron, S. M., 2020. Investigating
859 down-shore migration effects on individual growth and reproduction of the ecosystem engineer
860 *Arenicola marina*. *J. Mar. Sys.* 211(5): 103420. [https://doi.org/10.1016/j.jmarsys.2020.](https://doi.org/10.1016/j.jmarsys.2020.103420)
861 [103420](https://doi.org/10.1016/j.jmarsys.2020.103420)
- 862 De Vlas, J., 1979. Secondary production by tail regeneration in a tidal flat population of
863 lugworms (*Arenicola marina*), cropped by flatfish. *Netherlands J. Sea Res.* 13, 362–393.
864 [https://doi.org/10.1016/0077-7579\(79\)90012-7](https://doi.org/10.1016/0077-7579(79)90012-7)
- 865 Donadi, S., van der Heide, T., Piersma, T., van der Zee, E.M., Weerman, E.J., van de Koppel,
866 J., Olf, H., Devine, C., Hernawan, U.E., Boers, M., Planthof, L., Klemens Eriksson, B., 2015.
867 Multi-scale habitat modification by coexisting ecosystem engineers drives spatial separation
868 of macrobenthic functional groups. *Oikos* 124, 1502–1510. <https://doi.org/10.1111/oik.02100>

- 1
2
3
4
5
6
7
8
9
10
11
12
13
14
15
16
17
18
19
20
21
22
23
24
25
26
27
28
29
30
31
32
33
34
35
36
37
38
39
40
41
42
43
44
45
46
47
48
49
50
51
52
53
54
55
56
57
58
59
60
61
62
63
64
65
- 869 Ellien, C., Thiébaud, E., Dumas, F., Salomon, J. C., Nival, P. (2004). A modelling study of the
870 respective role of hydrodynamic processes and larval mortality on larval dispersal and recruit-
871 ment of benthic invertebrates: Example of *Pectinaria koreni* (Annelida: Polychaeta) in the
872 Bay of Seine (English Channel). *J. Plankton Res.* 26(2), 117–132. [https://doi.org/10.1093](https://doi.org/10.1093/plankt/fbh018)
873 [/plankt/fbh018](https://doi.org/10.1093/plankt/fbh018)
- 874 Failletaz, R., 2015. Estimation des capacités comportementales des larves de poissons et leurs
875 implications pour la phase larvaire. Université Pierre et Marie Curie - Paris 6. Ph D Thesis.
- 876 FAO, 2012. Recreational fisheries, FAO Technical Guidelines for Responsible Fisheries.
877 Rome.
- 878 Farke, H., Berghuis, E.M., 1979a. Spawning, larval development and migration of *Arenicola*
879 *marina* under field conditions in the western Wadden sea. *Netherlands J. Sea Res.* 13,
880 529–535.
- 881 Farke, H., Berghuis, E.M., 1979b. Spawning, larval development and migration behaviour of
882 *Arenicola marina* in the laboratory. *Netherlands J. Sea Res.* 13, 512–528.
- 883 Flach, E.C., Beukema, J.J., 1994. Density-governing mechanisms in populations of the lug-
884 worm *Arenicola marina* on tidal flats. *Mar. Ecol. Prog. Ser.* 115, 139–150. [https://doi.org/](https://doi.org/10.3354/meps115139)
885 [10.3354/meps115139](https://doi.org/10.3354/meps115139)
- 886 Grimm, V., 1999. Ten years of individual-based modelling in ecology: what have we learned
887 and what could we learn in the future? *Ecol. Model.* 115: 129–148
- 888 Grimm, V., Railsback, S. F., Vincenot, C. E., Berger, U., Gallagher, C., Deangelis, D.
889 L., Edmonds, B., Ge, J., Giske, J., Groeneveld, J., Johnston, A. S. A., Milles, A., Nabe-
890 Nielsen, J., Polhill, J. G., Radchuk, V., Rohwäder, M. S., Stillman, R. A., Thiele, J. C.,
891 Ayllón, D., 2020. The ODD protocol for describing agent-based and other simulation mod-
892 els: A second update to improve clarity, replication, and structural realism. *Jasss*, 23(2).
893 <https://doi.org/10.18564/jasss.4259>
- 894 Haberle, I., Bavčević, L., Tin Klanjscek, T., 2023. Fish condition as an indicator of stock
895 status: Insights from condition index in a food-limiting environment. *Fish. Fish.* 24(4)
896 <https://doi.org/10.1111/faf.12744>
- 897 Halpern, B. S., Frazier, M., Potapenko, J., Casey, K. S., Koenig, K., Longo, C., Lowndes, J.
898 S., Rockwood, R. C., Selig, E. R., Selkoe, K. A., Walbridge, S., 2015. Spatial and temporal
899 changes in cumulative human impacts on the world’s ocean. *Nature Communications*, 6,
900 7615. <https://doi.org/10.1038/ncomms8615>

- 1
2
3
4
5
6
7
8
9
10
11
12
13
14
15
16
17
18
19
20
21
22
23
24
25
26
27
28
29
30
31
32
33
34
35
36
37
38
39
40
41
42
43
44
45
46
47
48
49
50
51
52
53
54
55
56
57
58
59
60
61
62
63
64
65
- 901 Harley, C. D. G., Hughes, A. R., Hultgren, K. M., Miner, B. G., Sorte, C. J. B., Thorn-
902 ber, C. S., Rodriguez, L. F., Tomanek, L., Williams, S. L., 2006. The impacts of climate
903 change in coastal marine systems. *Ecol. Lett.*, 9(2), 228–241. [https://doi.org/10.1111/j.1461-](https://doi.org/10.1111/j.1461-0248.2005.00871.x)
904 [0248.2005.00871.x](https://doi.org/10.1111/j.1461-0248.2005.00871.x)
- 905 Hastings, A., 2013. Population Dynamics. *Encyclopedia of Biodiversity: Second Edition*, 6,
906 175–181. <https://doi.org/10.1016/B978-0-12-384719-5.00115-5>
- 907 Hedgecock, D., Barber, P., Edmands, S., 2007. Genetic approaches to measuring connectivity.
908 *Oceanography*, 20:70–79
- 909 Holmes, E.E., Lewis, M.A., Banks, J.E., Veit, R.R., 1994. Partial differential equations in
910 ecology: spatial interactions and population dynamics. *Ecology* 75: 17–29.
- 911 Howie, D., 1984. The reproductive biology of the lugworm, *Arenicola marina* L. *Fortschritte*
912 *Der Zoologie*, 29, 247–263.
- 913 Huret, M., Tsiaras, K., Daewel, U., Skogen, M. D., Gatti, P., Petitgas, P., Somarakis, S.,
914 2018. Variation in life-history traits of European anchovy along a latitudinal gradient: A
915 bioenergetics modelling approach. *MEPS*, 2018(May). <https://doi.org/10.3354/meps12574>
- 916 Huston, M.A., De Angelis, D.L., Post, W.M., 1988. New computer models unify ecological
917 theory. *BioSci.* 38: 682–691.
- 918 IPCC, 2021: Climate Change 2021: The Physical Science Basis. Contribution of Work-
919 ing Group I to the Sixth Assessment Report of the Intergovernmental Panel on Climate
920 Change[Masson-Delmotte, V., P. Zhai, A. Pirani, S.L. Connors, C. Péan, S. Berger, N. Caud,
921 Y. Chen, L. Goldfarb, M.I. Gomis, M. Huang, K. Leitzell, E. Lonnoy, J.B.R. Matthews, T.K.
922 Maycock, T. Waterfield, O. Yelekçi, R. Yu, and B. Zhou (eds.)]. Cambridge University Press,
923 Cambridge, United Kingdom and New York, NY, USA, doi:10.1017/9781009157896.
- 924 Kearney, M., Shine, R., Porter, W.P., 2009. The potential for behavioral thermoregulation
925 to buffer ““ cold-blooded ”” animals against climate warming. *PNAS* 106, 3835–3840.
- 926 Kearney, M., Simpson, S.J., Raubenheimer, D., Helmuth, B., 2010. Modelling the ecological
927 niche from functional traits. *Philos. Trans. R. Soc. Lond. B. Biol. Sci.* 365, 3469–3483.
928 <https://doi.org/10.1098/rstb.2010.0034>
- 929 Koch, J., De Schampelaere, K. A. C. (2020). Estimating inter-individual variability of
930 dynamic energy budget model parameters for the copepod *Nitocra spinipes* from existing life-
931 history data. *Ecol. Model.* 431, 109091. <https://doi.org/10.1016/j.ecolmodel.2020.109091>
- 932 Kooijman, S. A. L. M., 2014. Metabolic acceleration in animal ontogeny: An evolutionary
933 perspective. *J. Sea Res.*, 94, 128–137. <https://doi.org/10.1016/j.seares.2014.06.005>

- 1
2
3
4
5
6
7
8
9
10
11
12
13
14
15
16
17
18
19
20
21
22
23
24
25
26
27
28
29
30
31
32
33
34
35
36
37
38
39
40
41
42
43
44
45
46
47
48
49
50
51
52
53
54
55
56
57
58
59
60
61
62
63
64
65
- 934 Kooijman, S.A.L.M., 2010. Dynamic energy budget theory for metabolic organisation. Cambridge University Press.
- 935
- 936 Kosche, K., 2007. The influence of current velocity, tidal height and the lugworm *Arenicola marina* on two species of seagrass, *Zostera marina* L. and *Z. noltii* Hornemann. Bremen University.
- 937
938
- 939 Kristensen, E., 2001. Impact of polychaetes (*Nereis* spp. and *Arenicola marina*) on carbon biogeochemistry in coastal marine sediments. *Geochem. Trans.* 2, 92–103. <https://doi.org/10.1186/1467-4866-2-92>
- 940
941
- 942 Lewin, R. (1986). Supply-side ecology. *Science*, 234:25–27.
- 943
- 944 Luttikhuisen, P.C., Dekker, R., 2010. Pseudo-cryptic species *Arenicola defodiens* and *Arenicola marina* (Polychaeta: Arenicolidae) in Wadden Sea, North Sea and Skagerrak: Morphological and molecular variation. *J. Sea Res.* 63, 17–23. <https://doi.org/10.1016/j.seares.2009.09.001>
- 945
946
- 947 Malishev, M., Bull, M.C., Kearney, M.R., 2017. An individual-based model of ectotherm movement integrating metabolic and microclimatic constraints. *Methods Ecol. Evol.* 9, 472–489. <https://doi.org/10.1111/ijlh.12426>
- 948
949
- 950 Mangano, M. C., Giacoletti, A., Sarà, G., 2019. Dynamic Energy Budget provides mechanistic derived quantities to implement the ecosystem based management approach. *Journal of Sea Research*, 143, 272–279. <https://doi.org/10.1016/j.seares.2018.05.009>
- 951
952
- 953 Mangano, M. C., Mieszkowska, N., Helmuth, B., Domingos, T., Sousa, T., Baiamonte, G., Bazan, G., Cuttitta, A., Fiorentino, F., Giacoletti, A., Johnson, M., Lucido, G. D., Triantafyllou, G., 2020. Moving Toward a Strategy for Addressing Climate Displacement of Marine Resources: A Proof-of-Concept. *Frontiers in Marine Science*, 7, 1–16. <https://doi.org/10.3389/fmars.2020.00408>
- 954
955
956
957
- 958 Marques, G. M., Augustine, S., Lika, K., Pecquerie, L., Domingos, T., Kooijman, S. A. L. M., 2018. The AmP project: Comparing species on the basis of dynamic energy budget parameters. *PLoS Comput. Biol.*, 14(5), 1–23. <https://doi.org/10.1371/journal.pcbi.1006100>
- 959
960
- 961 Martin, B.T., Zimmer, E.I., Grimm, V., Jager, T., 2012. Dynamic Energy Budget theory meets individual-based modelling: A generic and accessible implementation. *Methods Ecol. Evol.* 3, 445–449. <https://doi.org/10.1111/j.2041-210X.2011.00168.x>
- 962
963
- 964 Matyja, K., 2023. Standard dynamic energy budget model parameter sensitivity. *Ecol. Model.* 478:110304. <https://doi.org/10.1016/j.ecolmodel.2023.110304>.
- 965

1
2
3
4
5
6
7
8
9
10
11
12
13
14
15
16
17
18
19
20
21
22
23
24
25
26
27
28
29
30
31
32
33
34
35
36
37
38
39
40
41
42
43
44
45
46
47
48
49
50
51
52
53
54
55
56
57
58
59
60
61
62
63
64
65

966 Newell, G.E., 1949. The later larval life of *Arenicola marina*. J. Mar. Biol. Assoc. UK 28,
967 635–639. <https://doi.org/https://doi.org/10.1017/S0025315400023456>

968 Newell, G.E., 1948. A contribution to our knowledge of the life history of *Arenicola marina*
969 L. J. Mar. Biol. Assoc. UK 27, 554–580. <https://doi.org/10.1017/S0025315400056022>

970 Olive, P.J.W., 1993. Management of the exploitation of the lugworm *Arenicola marina*
971 and the ragworm *Nereis virens* (Polychaeta) in conservation areas. Aquat. Conserv. Mar.
972 Freshw. Ecosyst. 3, 1–24. <https://doi.org/10.1002/aqc.3270030102>

973 Pethybridge, H., Roos, D., Loizeau, V., Pecquerie, L., Bacher, C., 2013. Responses of
974 European anchovy vital rates and population growth to environmental fluctuations : An
975 individual-based modeling approach. Ecol. Modell. 250, 370–383. <https://doi.org/10.1016/j.ecolmodel.2012.11.017>

977 Picard, N., Liang, J., 2014. Matrix models for size-structured populations: Unrealistic fast
978 growth or simply diffusion? PLoS ONE, 9(6). <https://doi.org/10.1371/journal.pone.0098254>

979 Pires, A., Martins, R., Magalhães, L., Soares, A., Figueira, E., Quintino, V., Rodrigues, A.,
980 Freitas, R., 2015. Expansion of lugworms towards southern European habitats and their
981 identification using combined ecological, morphological and genetic approaches. Mar. Ecol.
982 Prog. Ser. 533, 177–190. <https://doi.org/10.3354/meps11315>

983 Raimonet, M., Thieu, V., Silvestre, M., Oudin, L., Rabouille, C., Vautard, R., Garnier, J.,
984 2018. Landward perspective of coastal eutrophication potential under future climate change:
985 The Seine River case (France). Front. Mar. Sci., 5, 1–16. <https://doi.org/10.3389/fmars.2018.00136>

987 Reise, K., 1985. Tidal flat ecology - An experimental approach to species interactions, Eco-
988 logical Studies 54. 316 pp.

989 Reise, K., Simon, M., Herre, E., 2001. Density-dependent recruitment after winter distur-
990 bance on tidal flats by the lugworm *Arenicola marina*. Helgol. Mar. Res. 55, 161–165.
991 <https://doi.org/10.1007/s101520100076>

992 Ritter, F. E., Schoelles, M. J., Quigley, K. S., 2011. Determining the number of simulation
993 runs: treating simulations as theories by not sampling their behavior. In Human-in-the-Loop
994 Simulations (pp. 97–116). <https://doi.org/10.1007/978-0-85729-883-6>

995 Schöttler, U., 1989. Anaerobic metabolism in the lugworm *Arenicola marina* during low tide:
996 the influence of developing reproductive cells. Comp. Biochem. Physiol. , 92A(I), 1–7.

- 1
2
3
4
5
6
7
8
9
10
11
12
13
14
15
16
17
18
19
20
21
22
23
24
25
26
27
28
29
30
31
32
33
34
35
36
37
38
39
40
41
42
43
44
45
46
47
48
49
50
51
52
53
54
55
56
57
58
59
60
61
62
63
64
65
- 997 Schröer, M., Wittmann, A. C., Grüner, N., Steeger, H. U., Bock, C., Paul, R., Pörtner,
998 H. O., 2009. Oxygen limited thermal tolerance and performance in the lugworm *Areni-*
999 *cola marina*: A latitudinal comparison. *J. Exp. Mar. Biol. Ecol.*, 372(1–2), 22–30.
1000 <https://doi.org/10.1016/j.jembe.2009.02.001>
- 1001 Senga Green, D., Boots, B., Sigwart, J., Jiang, S., Rocha, C., 2016. Effects of conventional
1002 and biodegradable microplastics on a marine ecosystem engineer (*Arenicola marina*) and
1003 sediment nutrient cycling. *Environ. Pollut.* 208, 426–434. [https://doi.org/10.1016/j.envpol.](https://doi.org/10.1016/j.envpol.2015.10.010)
1004 [2015.10.010](https://doi.org/10.1016/j.envpol.2015.10.010)
- 1005 Then, A. Y., Hoenig, J. M., Hall, N. G., Hewitt, D. A., 2015. Evaluating the predictive
1006 performance of empirical estimators of natural mortality rate using information on over 200
1007 fish species. *CES J. Mar. Sci.* 72(1), 82–92. <https://doi.org/10.2307/4451538>
- 1008 Thomas, Y., Bacher, C., 2018. Assessing the sensitivity of bivalve populations to global
1009 warming using an individual-based modelling approach. *Glob. Chang. Biol.* 24, 4581–4597.
1010 <https://doi.org/10.1111/gcb.14402>
- 1011 Thomas, Y., Razafimahefa, N. R., Ménesguen, A., Bacher, C., 2020. Multi-scale interaction
1012 processes modulate the population response of a benthic species to global warming. *Ecol.*
1013 *Mod.*, 436 (March), 109295. <https://doi.org/10.1016/j.ecolmodel.2020.109295>
- 1014 Van De Wolfshaar, K. E., Barbut, L., Lacroix, G., 2021. From spawning to first-year recruit-
1015 ment: the fate of juvenile sole growth and survival under future climate conditions in the
1016 North Sea. *ICES J. Mar. Sci.* <https://doi.org/10.1093/icesjms/fsab025>
- 1017 Violle, C., Navas, M.-L., Vile, D., Kazakou, E., Fortunel, C., Hummel, I., Garnier, E.,
1018 2007. Let the concept of trait be functional!. *Oikos* 116, 882–892. [https://doi.org/10.1111/](https://doi.org/10.1111/j.2007.0030-1299.15559.x)
1019 [j.2007.0030-1299.15559.x](https://doi.org/10.1111/j.2007.0030-1299.15559.x).
- 1020 Volkenborn, N., 2005. Ecosystem engineering in intertidal sand by the lugworm *Arenicola*
1021 *marina*. University of Bremen. Ph D Thesis.
- 1022 Volkenborn, N., Reise, K., 2007. Effects of *Arenicola marina* on polychaete functional di-
1023 versity revealed by large-scale experimental lugworm exclusion. *J. Sea Res.* 57(1), 78–88.
1024 <https://doi.org/10.1016/j.seares.2006.08.002>
- 1025 Watson, G. J., Bentley, M. G., 1997. Evidence for a coelomic maturation factor controlling
1026 oocyte maturation in the polychaete *Arenicola marina* (L). *Invertebr. Reprod. Dev.*, 31(1–3),
1027 297–305. <https://doi.org/10.1080/07924259.1997.9672589>
- 1028 Watson, G.J., Cadman, P.S., Paterson, L.A., Bentley, M.G., Auckland, M.F., 1998. Control
1029 of oocyte maturation, sperm activation and spawning in two lugworm spec-ies: *Arenicola ma-*

1
2
3
4
5
6
7
8
9
10
11
12
13
14
15
16
17
18
19
20
21
22
23
24
25
26
27
28
29
30
31
32
33
34
35
36
37
38
39
40
41
42
43
44
45
46
47
48
49
50
51
52
53
54
55
56
57
58
59
60
61
62
63
64
65

1030 *rina* and *A. defodiens*. Mar. Ecol. Prog. Ser. 175, 167–176. <https://doi.org/10.3354/meps>
1031 175167

1032 Watson, G.J., Williams, M.E., Bentley, M.G., 2000. Can synchronous spawning be predicted
1033 from environmental parameters? A case study of the lugworm *Arenicola marina*. Mar. Biol.
1034 136, 1003–1017.

1035 Watson, G.J., Murray, J.M., Schaefer, M., Bonner, A., 2017. Bait worms: a valuable and
1036 important fishery with implications for fisheries and conservation management. Fish Fish.
1037 18, 374–388. <https://doi.org/10.1111/faf.12178>

1038 Wethey, D.S., Woodin, S. A., 2022. Climate change and *Arenicola marina*: Heat waves and
1039 the southern limit of an ecosystem engineer. Estuar. Coast. Shelf Sci. 276(15):108015 DOI:
1040 10.1016/j.ecss.2022.108015

1041 Wethey, D.S., Woodin, S.A., Hilbish, T.J., Jones, S.J., Lima, F.P., Brannock, P.M., 2011. Re-
1042 sponse of intertidal populations to climate: Effects of extreme events versus long term change.
1043 J. Exp. Mar. Biol. Ecol., 400(1–2), 132–144. <https://doi.org/10.1016/j.jembe.2011.02.008>

1044 Wrede, A., Andresen, H., Asmus, R., Wiltshire, K. H., Brey, T., 2019. Macrofaunal irrigation
1045 traits enhance predictability of nutrient fluxes across the sediment-water interface. Marine
1046 Ecology Progress Series, 632(2004), 27–42. <https://doi.org/10.3354/meps13165>

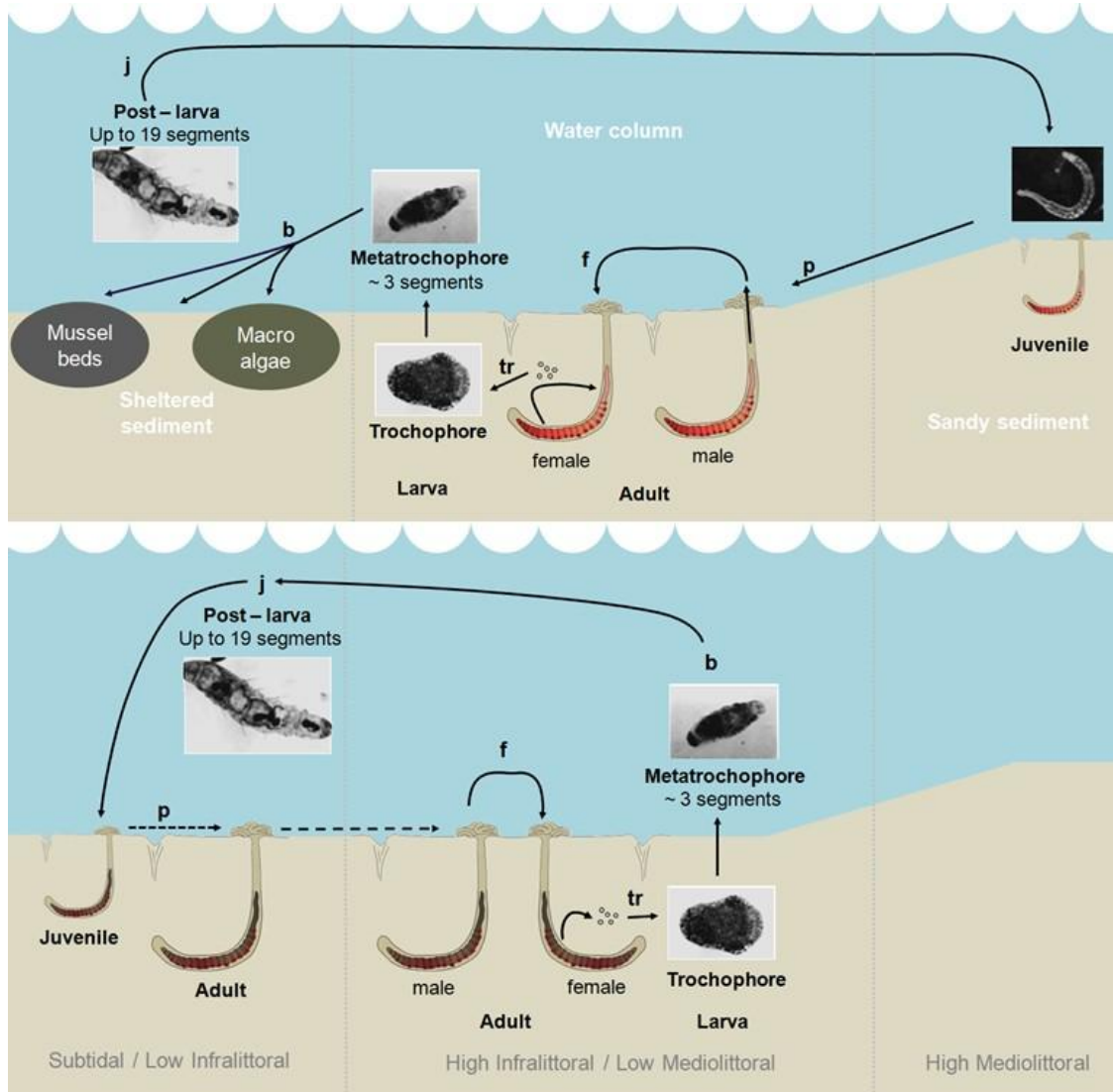
1047 Wright, S. 1931. Evolution in Mendelian populations. Genetics, 97, 97–159.

1048 Xenarios, S., Queiroga, H., Lillebø, A., Aleixo, A., 2018. Introducing a regulatory policy
1049 framework of bait fishing in European Coastal Lagoons: The case of Ria de Aveiro in Portugal.
1050 Fishes 3, 2. <https://doi.org/10.3390/fishes3010002>

1051 Yeakel, J. D., Pires, M. M., Aguiar, M. A. M. De, Donnell, J. L. O., Jr, P. R. G., Gravel,
1052 D., Gross, T., 2020. Diverse interactions and ecosystem engineering can stabilize community
1053 assembly. Nature Communications, 1–10. <https://doi.org/10.1038/s41467-020-17164-x>

1054 **Supplementary Material**

1055 *Sup. Mat. 1 - Lifecycles and Dynamic Energy Budget*

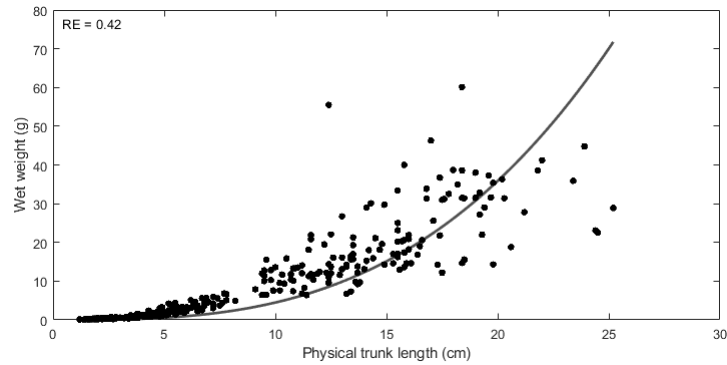


1056 Lifecycle of *Arenicola marina* (above), hypothesis on the lifecycle of *A. defodiens* and associated habi-
 1057 tats. Adapted from De Cubber et al. (2019), Farke and Berghuis (1979a, 1979b), Reise (1985) and Reise
 1058 et al. (2001). f stands for fertilization; tr for when the trochophore larva appears; b for birth (e.g. first
 1059 feeding, as described in the DEB theory); j for the end of metamorphosis; and p for puberty. Pictures of
 1060 the different life stages of *A. marina* are taken from Farke and Berghuis (1979a).

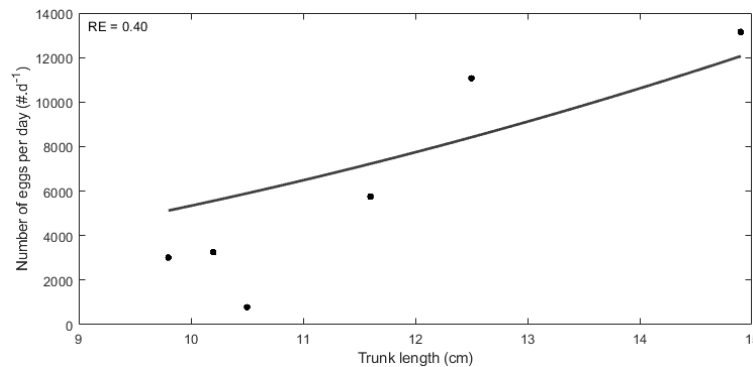
1061 *Sup. Mat. 2 - Estimation of DEB parameters for A. defodiens*

1062 **Sup. Mat. 2.1: Available data set for the parameter estimation of a DEB model for *Arenicola***
 1063 ***defodiens* and the associated prediction and relative error (RE) temperature, scaled functional**
 1064 **response and reference.**

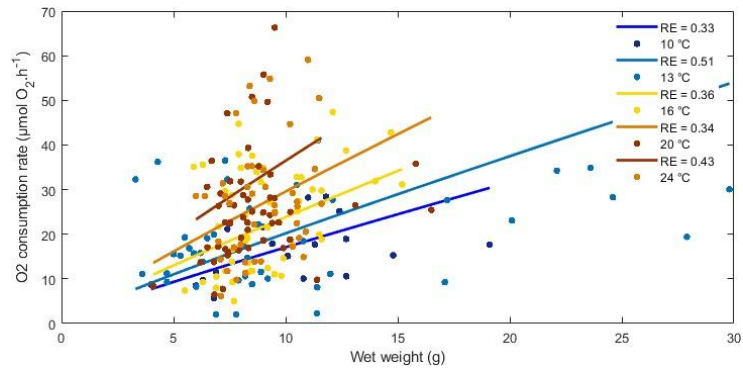
Type of data	Data	Symbol	Value	Prediction (RE)	Unit	Temperature (°C)	f	References
Zero-variate	age at trochophore larva	a_{tr}	3	3 (0.00)	d	13	1	De Cubber unpublished
	age at metamorphosis	a_j	90	90.21 (0.00)	d	12	1	Farke and Berghuis (1979)
	egg diameter	L_0	0.015	0.015 (0.001)	cm	-	1	De Cubber et al. (2018)
	length of the trochophore larva	L_{tr}	0.014	0.014 (0.00)	cm	-	1	De Cubber unpublished
	trunk length at puberty	TL_p	1.5	1.5 (0.00)	cm	-	1	Gaudron unpublished
	maximum trunk length	TL_i	25	23.84 (0.05)	cm	-	1	This study
	maximum wet weight	Ww_i	60	62 (0.03)	g	-	1	This study
	wet weight of an egg	Ww_0	$1.8 \cdot 10^{-6}$	$1.8 \cdot 10^{-6}$ (0.00)	g	-	1	De Cubber unpublished
Uni-variate	Length-Weight	TL-Ww	-	$g \cdot cm^{-1}$	-	-	0.8	This study
	Oxygen consumption	Ww-O2	-	-	$\mu mol O_2 \cdot h^{-1}$	10, 13, 16, 20, 24	0.8	This study
	Fecundity	TL-R	-	-	$oocytes \cdot year^{-1} \cdot cm^{-1}$	13	1	De Cubber unpublished



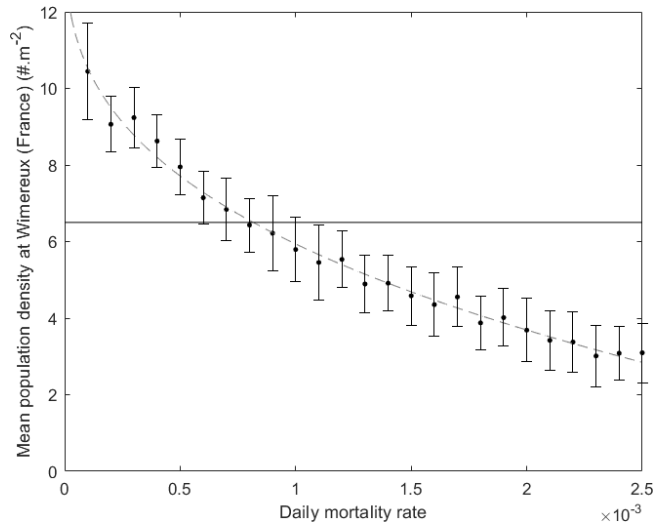
1065 **Sup. Mat. 2.2: Data (dots) and predictions (lines) of the wet weight as a function of trunk length**
 1066 **for *Arenicola defodiens* individuals collected in the Eastern English Channel (France) using an abj-DEB**
 1067 **model. The corresponding value of the shape coefficient is $\delta_M = 0.16$. RE stands for relative error.**



1068 **Sup. Mat. 2.3: Data (dots) and predictions (lines) of the number of oocytes produced per day as**
 1069 **a function of trunk length for *Arenicola defodiens* individuals collected in the Eastern English Channel**
 1070 **(France) using an abj-DEB model. RE stands for relative error.**

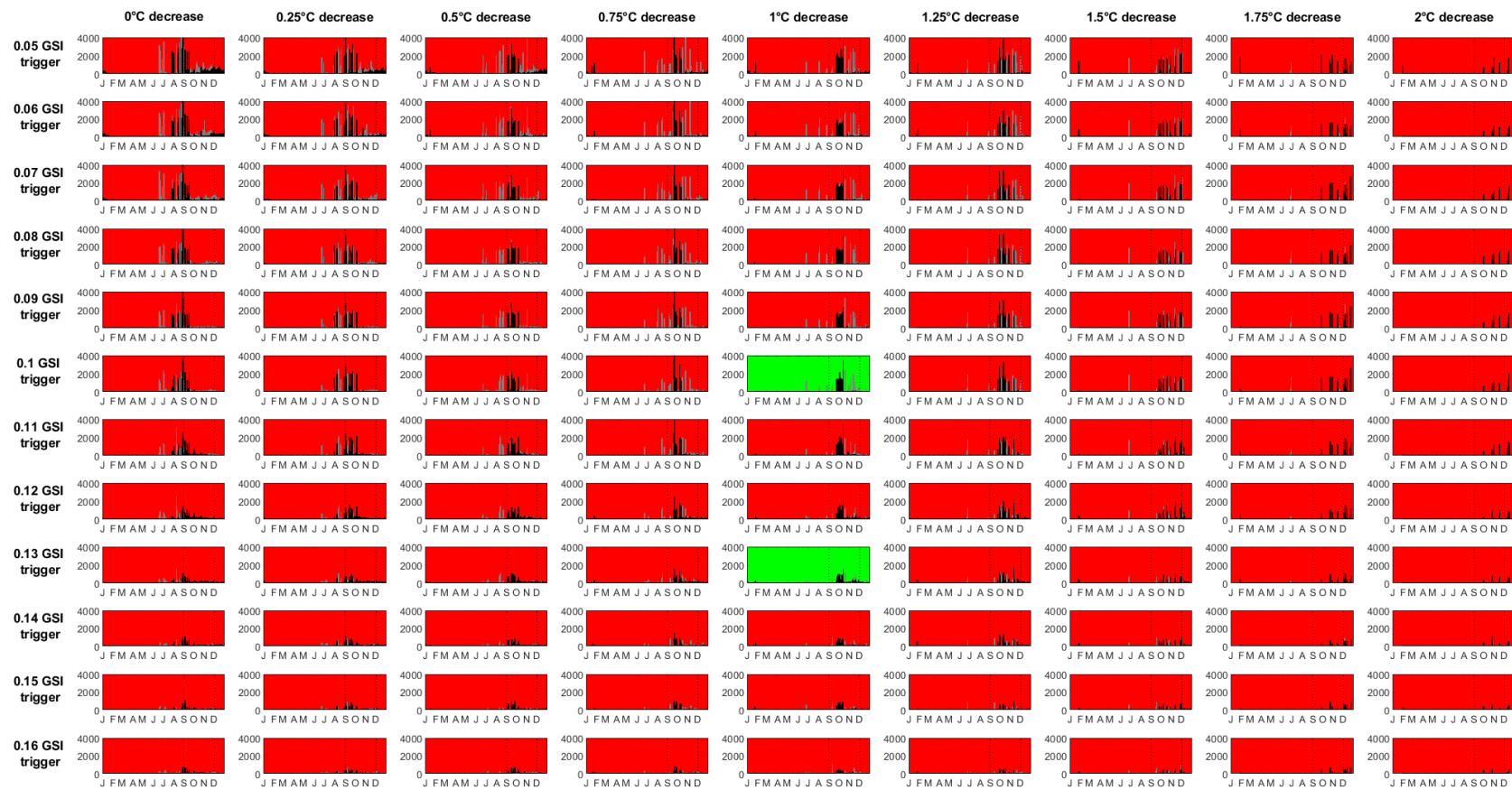


1
2
3
4
5
6
7
8
9
10
11
12
13
14
15
16
17
1071 Sup. Mat 2.4: Data (dots) and predictions (lines) of the oxygen consumption of the abj-DEB model
18
1072 of *Arenicola defodiens* measured by the authors as a function of wet weight at five different temperatures
19
1073 (from blue to red: 10, 13, 16, 20 and 24°C). The respective relative errors from 10 to 24°C were 0.33, 0.51,
20
21
1074 0.36, 0.34 and 0.43 with the abj-model.
22
23
24
25
26
27
28
29
30
31
32
33
34
35
36
37
38
39
40
41
42
43
44
45
46
47
48
49
50
51
52
53
54
55
56
57
58
59
60
61
62
63
64
65



1076 **Sup. Mat. 3.1: Mean and sd population density of *A. marina* at Wimereux (Wx, Easter**
 1077 **English Chanel, France) obtained with the IBM model according to various mortality rate values.**
 1078 **The fitted model (dotted grey line) for the relation between the mean population density at the**
 1079 **site and the daily mortality rate was (R^2 : 0.99): $Density \sim 14.42 \cdot 88.16 \cdot m^{-0.3389}$. The observed**
 1080 **Mean population density at Wx is represented by the horizontal line.**

1
2
3
4
5
6
7
8
9
10
11
12
13
14
15
16
17
18
19
20
21
22
23
24
25
26
27
28
29
30
31
32
33
34
35
36
37
38
39
40
41
42
43
44
45
46
47
48
49
50
51
52
53
54
55
56
57
58
59
60
61
62
63
64

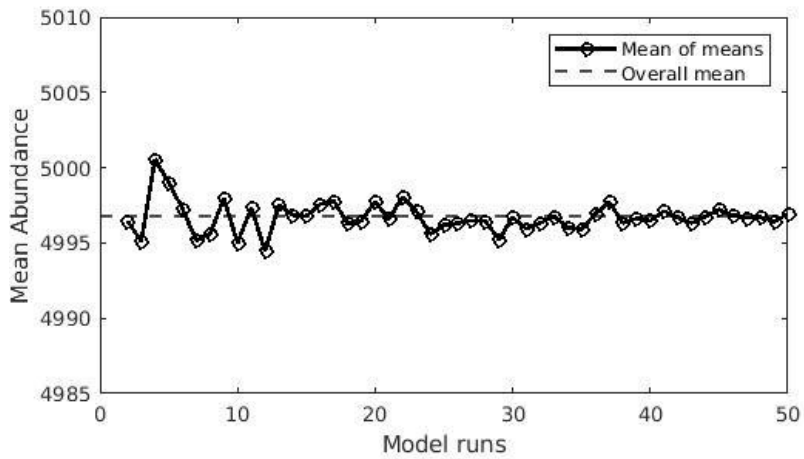
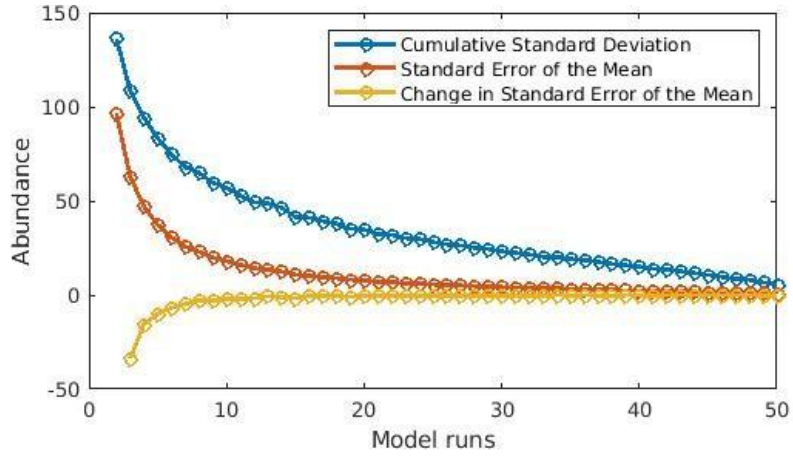


1081 Sup. Mat. 3.2: Output of the model in terms of number of individuals of *Arenicola marina* spawning per day along the year (from January J to December D) in France (black bars) and
 1082 Scotland (grey bars) with Sea-Surface Temperature decrease values from 0°C to 2°C over two weeks and GSI (wet weight of gametes over total wet weight of the individual) trigger values
 1083 between 0.05 and 0.16. Vertical dotted lines represent the main period of observation of spawning periods at both sites (De Cubber et al., 2018; Watson, 2000). Red backgrounds show that less
 1084 than 80% of the spawning events are simulated within this period, green backgrounds show that more than 80% of the spawning events are simulated within this period.

1085 *Sup. Mat. 4 - Location, coordinates and authors referring to Arenicola marina or A. defodiens's*
 1086 *occurrence used in this study.*

Num.	Location	Longitude	Latitude	Reference
*	Kandalashka Bay (Russia)	33.20126392	66.53614774	Pires et al. (2015)
1	Lindholmen (Sweden)	11.12555	58.8907333	Luttikhuizen and Dekker (2010)
*	Saltö (Sweden)	11.14779414	58.87222353	Luttikhuizen and Dekker (2010)
2	East Sands (St Andrews, Scotland)	-2.779435	56.338128	Watson and Bentley (1997)
3	Eden Estuary (St Andrews, Scotland)	-2.846838	56.363593	Watson and Bentley (1997)
4	Dunbar (Scotland)	-2.510515	56.002682	Watson and Bentley (1997)
5	Dorum-Neufeld (North Sea, Germany)	8.474212952	53.68955628	Schröer et al. (2009)
6	Slufter (Netherlands)	4.796710653	53.14159142	Luttikhuizen and Dekker (2010)
7	Eierlandse Gat (Wadden Sea, Netherlands)	4.971833333	53.1408833	Luttikhuizen and Dekker (2010)
8	Schorren (Wadden Sea, Netherlands)	4.90075	53.11675	Luttikhuizen and Dekker (2010)
9	Texel Beach (Netherlands)	4.764416667	53.119167	Luttikhuizen and Dekker (2010)
10	Mok (Wadden Sea, Netherlands)	4.760394598	53.00706617	Luttikhuizen and Dekker (2010)
11	Molenrak (Netherlands)	4.695916667	53.0159167	Luttikhuizen and Dekker (2010)
12	Malzwin (Wadden Sea, Netherlands)	4.903133333	52.9819667	Luttikhuizen and Dekker (2010)
13	Huiduinen (Netherlands)	4.717333333	52.9479167	Luttikhuizen and Dekker (2010)
14	Pembrey (Wales)	-4.256619	51.67684	Cadman and Nelson-Smith (1993)
15	Whiteford (Gower, Wales)	-4.251745	51.641174	Cadman and Nelson-Smith (1993)
16	Jersey Marine (Wales)	-3.855282	51.614809	Cadman and Nelson-Smith (1993)
*	Terneuzen (Netherlands)	3.796070515	51.34671156	Luttikhuizen and Dekker (2010)
17	Wimereux (France)	1.604804899	50.76702711	De Cubber et al. (2018)
18	Le Touquet (France)	1.576889725	50.5217217	De Cubber et al. (2018)
19	Fort Mahon (France)	1.5483621	50.34030109	De Cubber et al. (2018)
20	Ault (France)	1.451783331	50.11079353	De Cubber et al. (2018)
21	Roscoff (France)	-3.987793196	48.72783611	Pires et al. (2015)
*	Arcachon (France)	-1.1606092	44.66448716	Pires et al. (2015)
22	San Sebastian (Spain)	-1.976031	43.327907	Pires et al. (2015)
23	Viana do Castelo (Portugal)	-8.833605	41.677859	Pires et al. (2015)
24	Porto (Portugal)	-8.679619	41.151247	Pires et al. (2015)
25	Setubal (Portugal)	-8.925142	38.474085	Pires et al. (2015)
26	Vila Nova de Milfontes (Portugal)	-8.805631	37.783829	Pires et al. (2015)
27	Alvor (Portugal)	-8.597985	37.121745	Pires et al. (2015)
28	Cadiz (Spain)	-6.288526	36.60041	Pires et al. (2015)

* These sites were not kept in the study due to the bad quality on the environmental data extracted there (see Sup. Mat. 2 for further details).



1088 Evolution of standard deviation, standard error of the mean (*SEM*, with *SEM* $\propto \frac{1}{\sqrt{N}}$ and *dSEM* ?
 1089 (top panel) and mean of means (bottom panel) according to the number of model runs chosen.

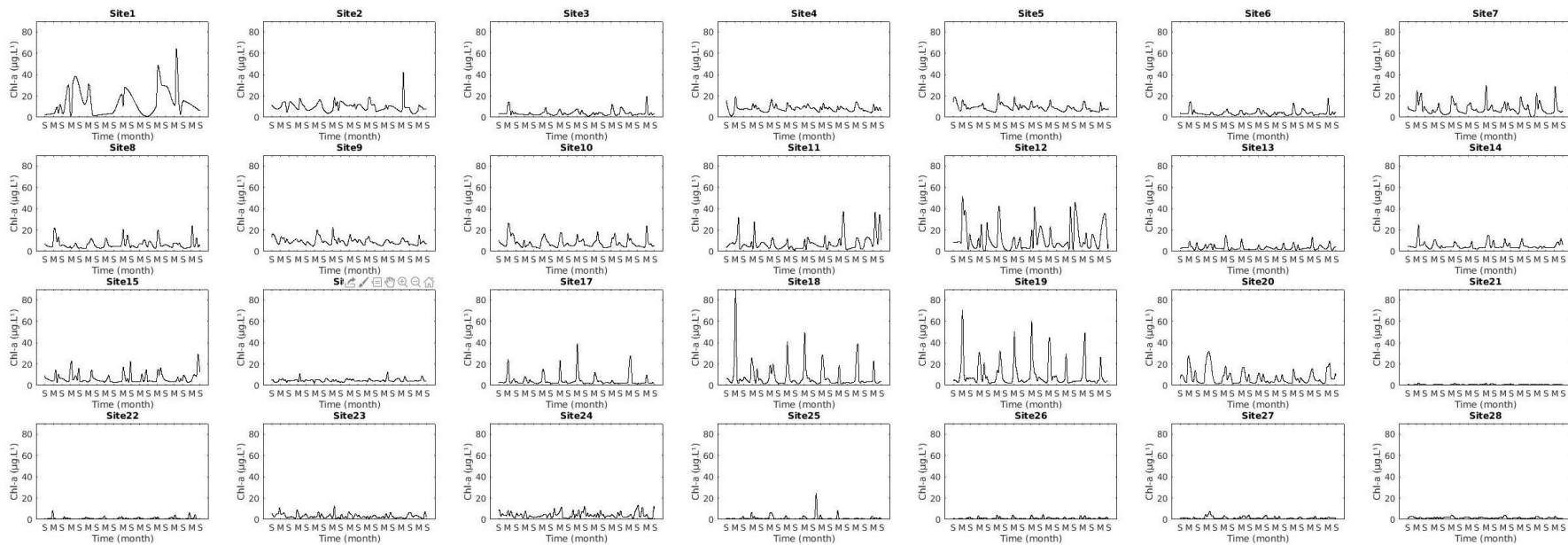
1
2
3
4
5
6
7
8
9
10
11
12
13
14
15
16
17
18
19
20
21
22
23
24
25
26
27
28
29
30
31
32
33
34
35
36
37
38
39
40
41
42
43
44
45
46
47
48
49
50
51
52
53
54
55
56
57
58
59
60
61
62
63
64

1090 *Sup. Mat. 6 - Mean values and associated of the biological traits at each sites and for each environmental scenario for the two species.*

Sites and scenarios	<i>Arenicola marina</i>						<i>Arenicola defodiens</i>				
	Abundance	TSB	Lp,pop	Lmax,pop	TRO	Abundance	TSB	Lp,pop	Lmax,pop	TRO	
1	6331 ~ 154	46789 ~ 1228	2.96 ~ 0.005	10.76 ~ 3.49	1.1 10 ⁹ ~ 1.6 10 ⁹	378 ~ 7	4912 ~ 212	1.51 ~ 0.003	12.34 ~ 0.17	1.4 10 ⁹ ~ 6.7 10 ⁸	
2	5448 ~ 186	37474 ~ 2185	2.97 ~ 0.003	11.31 ~ 3.60	1.6 10 ⁹ ~ 2.4 10 ⁹	0 ~ 0	0 ~ 0	0 ~ 0	0 ~ 0	0 ~ 1 0	
3	6164 ~ 275	37545 ~ 1868	2.93 ~ 0.003	9.33 ~ 1.29	4.2 10 ⁸ ~ 6.1 10 ⁸	393 ~ 8	3506 ~ 226	1.47 ~ 0.001	7.86 ~ 0.09	4.0 10 ⁸ ~ 1.5 10 ⁸	
4	4750 ~ 132	11434 ~ 460	2.96 ~ 0.006	11.25 ~ 3.31	1.5 10 ⁹ ~ 2.3 10 ⁹	410 ~ 4	1221 ~ 23	1.50 ~ 0	12.33 ~ 0.16	1.7 10 ⁹ ~ 6.2 10 ⁸	
5	6659 ~ 183	65607 ~ 3496	2.96 ~ 0.002	11.98 ~ 3.09	1.6 10 ⁹ ~ 2.4 10 ⁹	398 ~ 6	13692 ~ 234	1.51 ~ 0	13.16 ~ 0.17	2.1 10 ⁹ ~ 6.7 10 ⁸	
6	5702 ~ 155	19144 ~ 654	2.93 ~ 0.005	9.10 ~ 1.53	4.2 10 ⁸ ~ 6.1 10 ⁸	410 ~ 6	2483 ~ 75	1.48 ~ 0.001	8.09 ~ 0.12	4.5 10 ⁸ ~ 1.6 10 ⁸	
7	6604 ~ 198	56704 ~ 3604	2.96 ~ 0.004	11.04 ~ 2.67	1.0 10 ⁹ ~ 1.5 10 ⁹	398 ~ 5	11411 ~ 319	1.51 ~ 0.001	11.60 ~ 0.18	7.4 10 ⁸ ~ 4.3 10 ⁷	
8	6693 ~ 104	65233 ~ 2108	2.96 ~ 0.003	10.78 ~ 2.42	9.6 10 ⁸ ~ 1.4 10 ⁹	399 ~ 3	14764 ~ 433	1.50 ~ 0.001	10.65 ~ 0.13	1.1 10 ⁹ ~ 4.3 10 ⁸	
9	5679 ~ 205	19652 ~ 706	2.96 ~ 0.003	11.18 ~ 3.72	1.6 10 ⁹ ~ 2.5 10 ⁹	407 ~ 6	2697 ~ 75	1.51 ~ 0.001	13.29 ~ 0.09	2.2 10 ⁹ ~ 7.3 10 ⁸	
10	6225 ~ 151	39989 ~ 1624	2.96 ~ 0.004	10.72 ~ 3.17	1.2 10 ⁹ ~ 1.9 10 ⁹	401 ~ 8	6978 ~ 109	1.51 ~ 0.001	11.72 ~ 0.14	1.4 10 ⁸ ~ 4.7 10 ⁸	
11	5936 ~ 144	38816 ~ 1653	2.95 ~ 0.003	11.32 ~ 1.97	7.3 10 ⁸ ~ 1.1 10 ⁹	0 ~ 0	0 ~ 0	0 ~ 0	0 ~ 0	0 ~ 0	
12	6788 ~ 169	67794 ~ 2868	2.93 ~ 0.057	10.13 ~ 3.61	7.9 10 ⁸ ~ 1.2 10 ⁹	402 ~ 5	15046 ~ 430	1.51 ~ 0.004	6.72 ~ 0.29	5.5 10 ⁶ ~ 6.0 10 ⁵	
13	6619 ~ 188	52510 ~ 1859	2.91 ~ 0.003	9.06 ~ 0.82	2.3 10 ⁸ ~ 3.1 10 ⁸	395 ~ 5	9233 ~ 239	1.46 ~ 0.001	6.58 ~ 0.17	2.1 10 ⁸ ~ 5.9 10 ⁷	
14	6020 ~ 219	31853 ~ 1405	2.95 ~ 0.004	10.47 ~ 1.93	7.4 10 ⁸ ~ 1.1 10 ⁹	410 ~ 4	4795 ~ 221	1.49 ~ 0.002	9.35 ~ 0.11	7.6 10 ⁸ ~ 3.0 10 ⁸	
15	6280 ~ 132	42238 ~ 1552	2.95 ~ 0.004	10.47 ~ 2.76	9.7 10 ⁸ ~ 1.5 10 ⁹	400 ~ 9	6228 ~ 258	1.50 ~ 0.001	10.13 ~ 0.10	1.0 10 ⁹ ~ 3.9 10 ⁸	
16	6210 ~ 167	33438 ~ 1453	2.94 ~ 0.002	10.38 ~ 1.99	7.3 10 ⁸ ~ 1.1 10 ⁹	408 ~ 9	5516 ~ 109	1.48 ~ 0.001	9.62 ~ 0.14	7.9 10 ⁸ ~ 4.3 10 ⁸	
17	5376 ~ 125	16401 ~ 629	2.92 ~ 0.005	9.24 ~ 1.12	3.7 10 ⁸ ~ 5.3 10 ⁸	411 ~ 6	2273 ~ 35	1.47 ~ 0.002	7.26 ~ 0.07	3.5 10 ⁸ ~ 1.2 10 ⁸	
18	5819 ~ 193	27023 ~ 1117	2.95 ~ 0.006	10.00 ~ 1.97	6.6 10 ⁸ ~ 9.9 10 ⁸	412 ~ 3	2792 ~ 64	1.49 ~ 0.002	8.33 ~ 0.22	5.6 10 ⁸ ~ 2.0 10 ⁸	
19	6140 ~ 172	40394 ~ 2003	2.96 ~ 0.003	10.82 ~ 2.41	1.1 10 ⁹ ~ 1.6 10 ⁹	402 ~ 6	5242 ~ 108	1.50 ~ 0.001	10.07 ~ 0.13	1.0 10 ⁹ ~ 3.7 10 ⁸	
20	6183 ~ 165	35094 ~ 1731	2.97 ~ 0.006	10.04 ~ 2.23	9.1 10 ⁸ ~ 1.4 10 ⁹	404 ~ 7	4018 ~ 143	1.50 ~ 0.001	9.27 ~ 0.21	8.7 10 ⁸ ~ 2.6 10 ⁸	
21	172 ~ 51	44 ~ 14	2.71 ~ 0.009	4.12 ~ 0.10	3.8 10 ⁶ ~ 9.0 10 ⁵	403 ~ 27	47 ~ 7	1.32 ~ 0.002	2.37 ~ 0.04	9.6 10 ⁷ ~ 1.7 10 ⁶	
22	97 ~ 50	10 ~ 6	2.56 ~ 0.038	3.33 ~ 0.10	2.1 10 ⁶ ~ 8.0 10 ⁵	0 ~ 0	0 ~ 0	0 ~ 0	0 ~ 0	0 ~ 0	
23	4885 ~ 144	10382 ~ 388	2.92 ~ 0.006	8.58 ~ 0.65	2.8 10 ⁸ ~ 3.9 10 ⁸	409 ~ 4	430 ~ 46	1.47 ~ 0.002	5.87 ~ 0.21	1.2 10 ⁸ ~ 5.4 10 ⁷	
24	5815 ~ 205	19082 ~ 1156	2.93 ~ 0.004	9.38 ~ 1.08	5.1 10 ⁸ ~ 7.4 10 ⁸	409 ~ 6	1513 ~ 135	1.47 ~ 0.003	6.89 ~ 0.15	2.5 10 ⁸ ~ 1.8 10 ⁸	
25	137 ~ 69	24 ~ 12	2.81 ~ 0.018	3.69 ~ 0.18	5.4 10 ⁶ ~ 1.0 10 ⁶	0 ~ 0	0 ~ 0	0 ~ 0	0 ~ 0	0 ~ 0	
26	150 ~ 76	29 ~ 16	2.68 ~ 0.024	3.94 ~ 0.16	6.0 10 ⁶ ~ 2.1 10 ⁶	1 ~ 1	0 ~ 0	1.38 ~ 0.001	1.68 ~ 0.5	2.0 10 ⁵ ~ 1.3 10 ⁵	
27	951 ~ 185	295 ~ 66	2.83 ~ 0.009	4.98 ~ 0.17	3.2 10 ⁷ ~ 4.0 10 ⁶	0 ~ 0	0 ~ 0	0 ~ 0	0 ~ 0	0 ~ 0	
28	2233 ~ 108	1250 ~ 162	2.84 ~ 0.008	5.67 ~ 0.18	5.2 10 ⁷ ~ 3.5 10 ⁷	0 ~ 0	0 ~ 0	0 ~ 0	0 ~ 0	0 ~ 0	
SST _r ,10 & chl-a _r ,1	93 ~ 51	23 ~ 14	2.72 ~ 0.012	4.04 ~ 0.13	2.6 10 ⁶ ~ 7.0 10 ⁵	369 ~ 80	15 ~ 4	1.34 ~ 0.002	2.50 ~ 0.05	9.1 10 ⁶ ~ 2.6 10 ⁶	
SST _r ,12 & chl-a _r ,1	135 ~ 80	34 ~ 22	2.71 ~ 0.012	4.07 ~ 0.17	3.6 10 ⁶ ~ 1.6 10 ⁶	388 ~ 84	15 ~ 3	1.33 ~ 0.004	2.37 ~ 0.04	9.6 10 ⁶ ~ 2.4 10 ⁶	
SST _r ,19 & chl-a _r ,1	214 ~ 83	57 ~ 23	2.70 ~ 0.012	4.25 ~ 0.12	5.7 10 ⁶ ~ 1.2 10 ⁶	375 ~ 59	14 ~ 2	1.32 ~ 0.005	2.25 ~ 0.04	5.1 10 ⁶ ~ 1.2 10 ⁶	
SST _r ,10 & chl-a _r ,5	5620 ~ 140	28351 ~ 1217	2.94 ~ 0.004	10.78 ~ 1.68	5.5 10 ⁸ ~ 8.1 10 ⁸	409 ~ 5	1039 ~ 33	1.49 ~ 0.001	9.71 ~ 0.09	6.7 10 ⁸ ~ 2.3 10 ⁸	
SST _r ,12 & chl-a _r ,5	5576 ~ 193	30672 ~ 1747	2.95 ~ 0.004	10.66 ~ 1.93	6.9 10 ⁸ ~ 1.0 10 ⁹	409 ~ 7	953 ~ 45	1.49 ~ 0.001	9.31 ~ 0.11	7.5 10 ⁸ ~ 2.9 10 ⁸	
SST _r ,19 & chl-a _r ,5	5702 ~ 245	35808 ~ 1955	2.96 ~ 0.003	11.27 ~ 1.70	1.0 10 ⁹ ~ 1.5 10 ⁹	407 ~ 5	968 ~ 17	1.50 ~ 0.002	9.43 ~ 0.16	1.2 10 ⁹ ~ 3.9 10 ⁸	
SST _r ,10 & chl-a _r ,14	6015 ~ 172	47344 ~ 2276	2.96 ~ 0.008	10.97 ~ 3.28	1.0 10 ⁹ ~ 1.5 10 ⁹	383 ~ 11	971 ~ 35	1.50 ~ 0.004	11.91 ~ 0.19	1.2 10 ⁹ ~ 6.0 10 ⁸	
SST _r ,12 & chl-a _r ,14	6003 ~ 213	50906 ~ 2460	2.96 ~ 0.007	10.39 ~ 4.09	1.2 10 ⁹ ~ 1.9 10 ⁹	371 ~ 12	949 ~ 33	1.50 ~ 0.002	12.17 ~ 0.20	1.3 10 ⁹ ~ 5.4 10 ⁸	
SST _r ,19 & chl-a _r ,14	5943 ~ 83	59212 ~ 1844	2.97 ~ 0.003	11.67 ~ 3.90	2.7 10 ⁹ ~ 2.7 10 ⁹	349 ~ 13	1115 ~ 36	1.50 ~ 0.002	13.00 ~ 0.13	1.4 10 ⁹ ~ 3.5 10 ⁸	

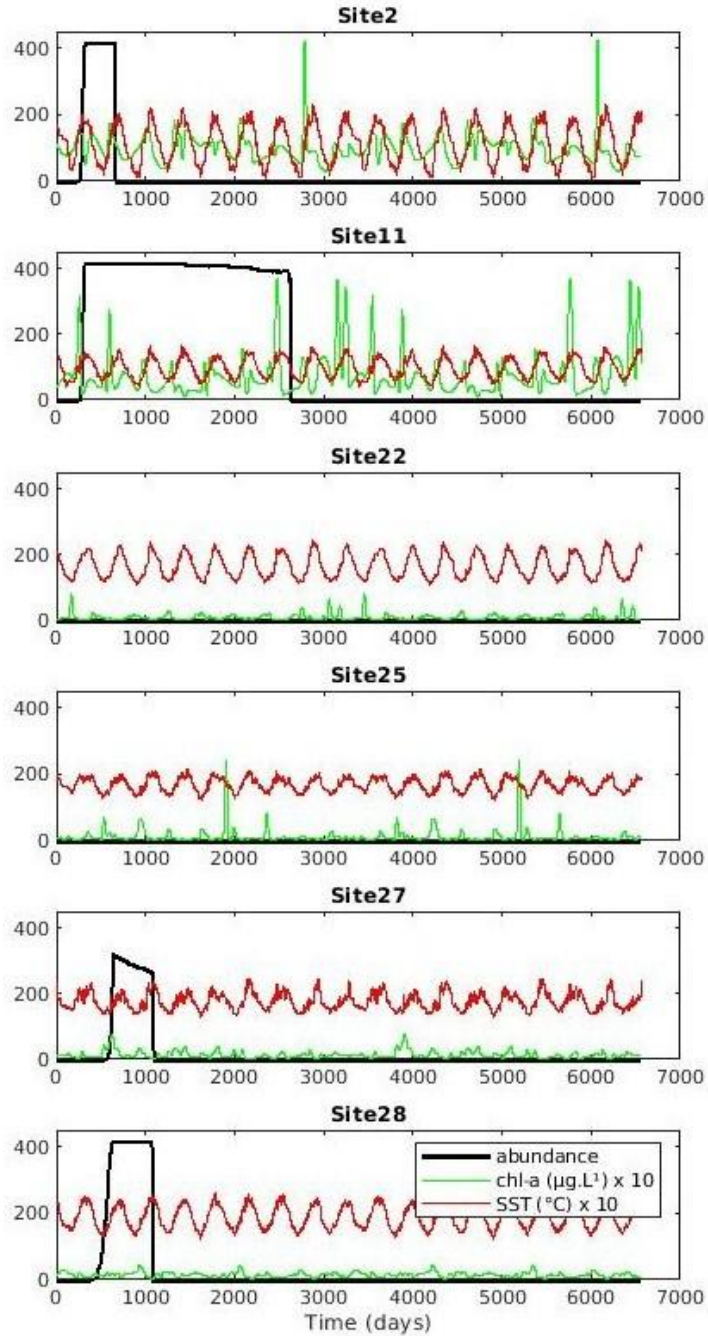
1
2
3
4
5
6
7
8
9
10
11
12
13
14
15
16
17
18
19
20
21
22
23
24
25
26
27
28
29
30
31
32
33
34
35
36
37
38
39
40
41
42
43
44
45
46
47
48
49
50
51
52
53
54
55
56
57
58
59
60
61
62
63
64

1093 *Sup. Mat. 7.2 - Interpolated time-series of chlorophyll-a concentrations ($\mu\text{g}\cdot\text{L}^{-1}$) at each study site (see Sup. Mat. 1 for correspondence between numbers*
 1094 *and sites) used further in the DEB-IBM for *Arenicola marina* and *A. defodiens*. Sites are ordered from the higher latitudes to the lower latitudes.*



1
2
3
4
5
6
7
8
9
10
11
12
13
14
15
16
17
18
19
20
21
22
23
24
25
26
27
28
29
30
31
32
33
34
35
36
37
38
39
40
41
42
43
44
45
46
47
48
49
50
51
52
53
54
55
56
57
58
59
60
61
62
63
64
65

1095 *Sup. Mat. 8 - A. defodiens' simulated abundance and associated chl-a and SST according to time*
1096 *(d) over the two cycles of 10 years at the 6 sites where populations were predicted to crash. Site*
1097 *numbers refer to Sup. Mat. 1.*



Declaration of interests

The authors declare that they have no known competing financial interests or personal relationships that could have appeared to influence the work reported in this paper.

The authors declare the following financial interests/personal relationships which may be considered as potential competing interests: